

Review

# Thermally Stable Carbon Materials from Polybenzoxazines: Structure, Properties, and Supercapacitor Potential

Thirukumaran Periyasamy <sup>†</sup>, Shakila Parveen Asrafali <sup>†</sup> and Jaewoong Lee <sup>\*</sup>

Department of Fiber System Engineering, Yeungnam University, Gyeongsan 38541, Republic of Korea

\* Correspondence: jaewlee@yu.ac.kr

† These authors contributed equally to this work.

**Abstract:** This review explores the structural and electrochemical characteristics of carbon materials derived from polybenzoxazines, emphasizing their potential in supercapacitors. A detailed analysis of thermal degradation by-products during carbonization reveals distinct competing mechanisms, underscoring the exceptional thermal stability of benzoxazines. These materials exhibit significant pseudocapacitive behavior and excellent charge retention, making them strong candidates for energy storage applications. The versatility of polybenzoxazine-based carbons enables the formation of diverse morphologies—nanospheres, foams, films, nanofibers, and aerogels—each tailored for specific functionalities. Advanced synthesis techniques allow for precise control over porosity at the nanoscale, optimizing performance for supercapacitors and beyond. Their exceptional thermal stability, electrical conductivity, and tunable porosity extend their utility to gas adsorption, catalysis, and electromagnetic shielding. Additionally, their intumescence properties (unique ability to expand when exposed to high heat) make them promising candidates for flame-retardant coatings. The combination of customizable architecture, superior electrochemical performance, and high thermal resistance highlights their transformative potential in sustainable energy solutions and advanced protective applications.



Academic Editors: Ruizhi Li and  
Hai Wang

Received: 13 March 2025

Revised: 27 March 2025

Accepted: 2 April 2025

Published: 4 April 2025

**Citation:** Periyasamy, T.; Asrafali, S.P.; Lee, J. Thermally Stable Carbon Materials from Polybenzoxazines: Structure, Properties, and Supercapacitor Potential. *Batteries* **2025**, *11*, 140. <https://doi.org/10.3390/batteries11040140>

**Copyright:** © 2025 by the authors. Licensee MDPI, Basel, Switzerland. This article is an open access article distributed under the terms and conditions of the Creative Commons Attribution (CC BY) license (<https://creativecommons.org/licenses/by/4.0/>).

**Keywords:** polybenzoxazine; carbon materials; porosity; supercapacitor; sustainable energy

## 1. Introduction

Carbon has played a significant role in human history, and has been utilized in a variety of applications for centuries. From its early use as a fuel source and an additive in iron production, to its function as an adsorbent and a component in lubricants, carbon has been indispensable. It has also been used in pencil cores and as gemstones for jewelry [1–3]. More recently, carbon has been engineered into advanced materials, such as carbon fibers, offering enhanced properties for various industrial applications. A major milestone in carbon research came with the theoretical prediction of a unique spherical carbon structure, C<sub>60</sub>, by Osawa in 1970. This prediction was experimentally validated when Kroto and colleagues discovered C<sub>60</sub> molecules in the soot produced from vaporized carbon under helium conditions [4,5]. This newly identified molecule was named Buckminsterfullerene, or “Buckyball”, as a tribute to the architect Buckminster Fuller, whose geodesic dome designs resembled the structure of the molecule. The discovery of fullerenes was groundbreaking, and contributed to earning a Nobel Prize, although astrophysicists had long been aware of these carbon structures in extraterrestrial environments. Fullerenes

exhibited intriguing physical properties, including electrical conductivity and magnetism. However, their applications were limited due to their small aspect ratio [6–8]. The significance of carbon materials expanded further when Iijima conducted a detailed investigation of an elongated version of the Buckyball, which became known as the carbon nanotube (CNT). Unlike fullerenes, CNTs possess a much higher aspect ratio, sometimes extending to hundreds, making them highly effective in reinforcing polymers, ceramics, and metal matrices. Since their discovery, both single-walled and multi-walled carbon nanotubes have been extensively studied for their exceptional strength and electrical properties. The evolution of carbon materials continued with the discovery of graphene, an atom-thick, two-dimensional carbon sheet. First isolated by Geim and Novoselov through the mechanical exfoliation of graphite, graphene quickly garnered attention, due to its exceptional electrical, thermal, and mechanical properties. This breakthrough resulted in another Nobel Prize in the field of carbon-based materials. However, producing graphene by peeling graphite layer by layer proved impractical for large-scale applications. This challenge led to the development of chemical exfoliation techniques, such as the Hummers method, which involves chemically modifying graphite into graphene oxide (GO). Though graphene oxide is less structurally ordered than mechanically exfoliated graphene, it still serves as an effective reinforcement material. However, its electrical conductivity is significantly lower than that of pristine graphene [9–13]. The field of advanced carbon materials is rapidly expanding, covering a wide range of structures, including single-walled carbon nanotubes (SWCNTs), multi-walled carbon nanotubes (MWCNTs), graphene derivatives, carbon-based supercapacitors, electrode materials, carbon quantum dots, metal-free carbon catalysts, and aerogels. Additionally, researchers are investigating emerging materials like graphane and graphene. A major challenge in this field is the high production cost, due to the lack of efficient mass-production techniques. Therefore, there is a strong academic and technological drive to develop cost-effective synthesis methods. One promising avenue is polybenzoxazine, a newly commercialized class of polymers that has revitalized thermoset research. This material provides exceptional molecular design versatility and a high char yield, making it ideal for carbon-related applications. This review examines both fundamental and applied research on benzoxazine resins and cross-linked polybenzoxazines in carbon material production [14–17]. Recently, the preparation and application of carbon materials derived from polybenzoxazines have been explored. Polybenzoxazines, synthesized from benzoxazine monomers or oligomeric precursors, undergo polymerization at elevated temperatures (140–240 °C), often with catalysts to enhance efficiency. These materials exhibit high char yields (35–75%), making them suitable for various carbonaceous structures, such as solid blocks, aerogels, monoliths, nanofibers, and carbon dots. This study highlights key synthesis methods, focusing on polymerization and carbonization conditions. It discusses solid structure formation, emphasizing the importance of solvent drying to prevent porosity. In aerogel development, the paper examines different drying techniques—supercritical drying, freeze-drying, and ambient drying—each of which influence the final pore structure. Freeze-drying provides controlled pore morphology, while nanofiller reinforcements enhance mechanical stability. The paper concludes that by selecting appropriate synthesis and drying techniques, polybenzoxazine-derived carbon materials can be tailored for applications in catalysis, adsorption, and energy storage. The findings provide insights into optimizing processing conditions to achieve desirable structural and functional properties [18]. This paper also explores the synthesis, properties, and applications of gel-based materials. It focuses on the structural characteristics and functionalization of gels for various advanced applications, including catalysis, adsorption, and energy storage. The study highlights different preparation techniques and the influence of drying methods on the final morphology and performance of the gels. Key findings

include the importance of precursor selection and processing conditions in tailoring pore structures and mechanical properties. The research provides insights into optimizing gel-based materials for industrial and scientific applications [19]. Furthermore, this study investigates the development of polymer-based carbon materials with high thermal and mechanical stability. It discusses synthesis pathways, emphasizing the polymerization and carbonization conditions that influence the final structure. The paper examines the role of catalysts and initiators in enhancing polymerization efficiency and reducing processing temperatures. Additionally, it explores different applications of these carbon-based materials, particularly in energy storage and catalysis. The findings suggest that controlled processing can lead to highly porous and efficient materials that are suitable for various high-performance applications [20].

The performance of supercapacitors (SCs) is strongly influenced by the carbon material's surface area, pore size, and distribution. Micropores boost electrical double-layer capacitance, mesopores improve ion transport by lowering resistance, and macropores act as reservoirs to streamline ion diffusion. Hierarchical porous structures combining micro-, meso-, and macropores provide a synergistic effect, optimizing ion accessibility and improving overall device performance. To enhance the specific energy of SCs, researchers have explored various strategies, including designing hybrid electrodes that combine EDLC with pseudocapacitance. While carbon-based materials contribute to EDLC, pseudocapacitance is provided by heteroatom-doped carbon materials and transition metal oxides. Heteroatom doping (e.g., nitrogen, sulfur, oxygen, and phosphorus) improves surface wettability, facilitates ion interactions, and enhances capacitive performance through reversible Faradaic reactions. Transition metal oxides, such as bimetal oxides, introduce additional active sites, further boosting capacitance and energy storage efficiency [21–25]. The choice of electrolyte also plays a crucial role in determining the electrochemical window and overall performance of SCs. Aqueous electrolytes offer high conductivity, but suffer from leakage issues, while organic and ionic liquid electrolytes provide a broader voltage range, but lower conductivity. Recent research has shown that redox-active electrolytes, such as iodide-based solutions, can significantly enhance capacitance and energy density through fast Faradaic reactions, contributing to improved charge storage capabilities. In addition to SCs, lithium-ion batteries (LIBs) remain a dominant energy storage technology, particularly for portable electronics and electric vehicles. Among various cathode materials, olivine-type LiFePO<sub>4</sub> has gained attention, due to its environmental compatibility, stable operating voltage, and excellent cycling performance. However, its intrinsic low electronic and ionic conductivity poses a challenge for practical applications [26–31]. To address this issue, strategies such as nano-structuring, porous architecture design, and conductive coatings (e.g., nitrogen-doped carbon layers) have been employed to enhance charge transport and storage efficiency. Recent advancements in carbon-based materials for energy storage have led to the development of novel three-dimensional (3D) graphene architectures. Graphene-based electrodes offer high surface areas, excellent electrical conductivity, and strong electrochemical stability, making them attractive candidates for next-generation SCs. However, challenges such as graphene sheet aggregation and restacking can hinder performance. To mitigate these issues, researchers have developed 3D cross-linked graphene structures, aerogels, and porous graphene films, which improve ion accessibility and prevent structural collapse during cycling. In instantaneous applications, continuous innovation in electrode materials, electrolyte selection, and device architecture is driving the advancement of high-performance SCs and LIBs. The integration of carbon-based materials, hierarchical porous structures, and redox-active electrolytes holds great promise for developing efficient, sustainable, and eco-friendly energy storage solutions. As research

progresses, these technologies are expected to play a critical role in meeting the growing energy demands of modern society [32–38].

## 2. Preparation of Carbon-Materials from Polybenzoxazines: Key Methods

Polybenzoxazines are synthesized from benzoxazine monomers or oligomeric precursors, including main-chain, side-chain, and telechelic types. The resulting polymer structure and properties depend on the precursor type. A comprehensive body of literature details various benzoxazine resins [12–14]. Benzoxazine monomers are synthesized through different approaches, with polymerization occurring at 140–240 °C, either thermally or with catalysts. While benzoxazine supports cationic ring-opening polymerization [28], catalysts like phenol impurities or benzoxazine oligomers enhance efficiency and lower reaction temperatures [20–23]. Figure 1 illustrates the general synthesis and polymerization scheme. Polybenzoxazines yield high char levels (35–75%), making them ideal for carbonaceous material production. The precursor formation and carbonization methods influence the final carbon material morphology, which may take the form of solid blocks, aerogels, monoliths, nanofibers, or carbon dots.

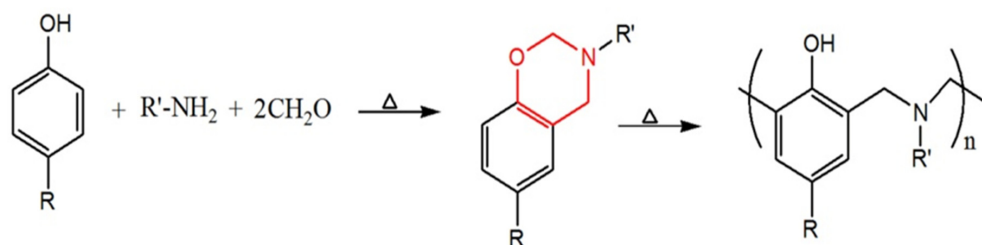


**Figure 1.** Synthesis of benzoxazine monomer from phenolic derivative and ring-opening polymerization of benzoxazine.

### 2.1. Formation of Solid Structures and Composites

Benzoxazine resins polymerize without by-product formation, enabling solid block fabrication. However, careful solvent drying is crucial, as benzoxazines retain solvents that can cause porosity if evaporated during polymerization. Additionally, monomer evaporation, particularly in low-viscosity benzoxazines, can lead to defects [24,25]. To mitigate this, AB-type benzoxazine monomers undergo a Diels–Alder reaction before polymerization, reducing volatility and increasing molecular weight, while maintaining low viscosity. Figure 2 illustrates this process.

### 2.2. Development of Carbon Aerogels

Aerogels, characterized by interconnected pores, are valuable in adsorption and catalysis applications. Originally documented by Kistler in 1931, carbon aerogels gained prominence in the 1990s [29]. A major challenge in aerogel synthesis is pore collapse due to capillary forces during drying. Supercritical drying minimizes these effects, but is expensive and has scalability limitations. Alternative methods include freeze-drying and ambient drying. Freeze-drying, widely used in industry, influences aerogel morphology through ice crystal formation, resulting in layered pore structures [23,31]. Ambient drying is more cost-effective, but requires strong polymer gels to prevent pore collapse. Polybenzoxazine aerogels have been successfully synthesized using both methods [35]. Studies indicate that supercritical CO<sub>2</sub> drying offers comparable outcomes to ambient drying for benzoxazine-derived aerogels. Pore structure and distribution in carbon aerogels can be tailored using surfactants that influence gel sphere aggregation, enhancing catalytic and adsorption properties. Freeze-drying provides additional control over pore

morphology, with ice matrix-induced layering reflected in the final carbonized structure (Figure 3) [22–24]. Reinforcement with montmorillonite nanoclay improves structural alignment, while nanofiller platelets further refine internal surface accessibility [36]. These synthesis and drying methods enable precise control over polybenzoxazine-derived carbon materials, facilitating their customization for various applications. Table 1 summarizes different methods for the synthesis of carbon-based materials, covering their performance, scalability, cost, and environmental impact.

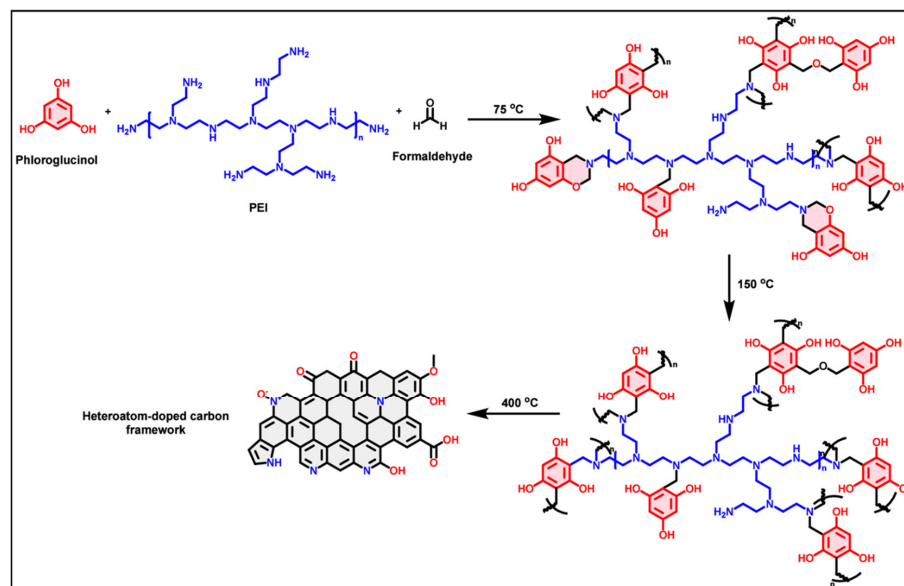


**Figure 2.** Synthesis route for heteroatom-doped carbon, using phloroglucinol, PEI, and formaldehyde as precursors [37].

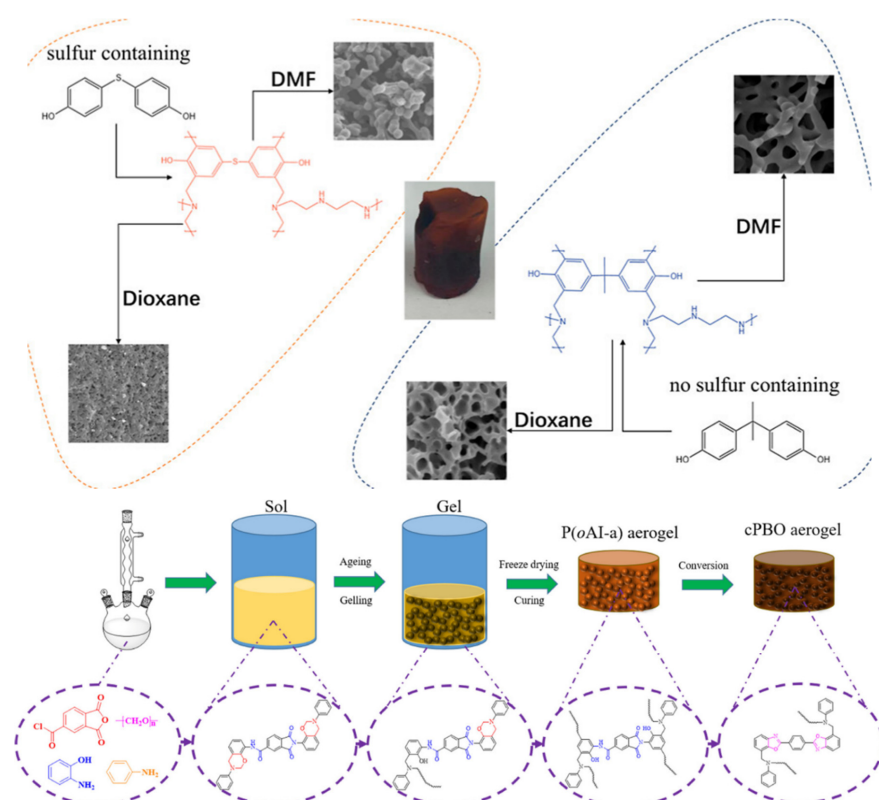


**Figure 3.** Schematic illustration of preparation and conversion process of cPBO aerogels, along with synthesis pathway of main-chain benzoxazine aerogel derived from TBP-TETA [36,38].

**Table 1.** Comparison of synthesis methods for carbon-based materials. Covers performance, scalability, cost, and environmental impact.

Synthesis Method	Performance	Scalability	Cost	Environmental Impact
Freeze-Drying	High porosity and surface area, beneficial for catalysis and adsorption.	Large-scale processing is possible, but energy-intensive.	High, due to freezing and sublimation energy costs.	High energy consumption but no hazardous solvents.
Surfactant-Assisted Synthesis	Precise pore control enhances electrochemical performance.	Requires additional surfactant removal steps, limiting scalability.	Moderate, depends on surfactant type and processing.	Potential waste disposal concerns from surfactants.
Template-Free Synthesis	Self-doped carbon materials exhibit large surface area and high electrochemical performance.	Simplified process, making it highly scalable.	Low, as it avoids the use of templates or surfactants.	More sustainable, avoids hazardous chemicals and additional processing steps.

### 3. Key Characteristics of Polybenzoxazines

#### 3.1. Thermal Decomposition and Carbon Residue Formation

Carbonization refers to the thermal decomposition of organic compounds to generate a carbon-rich residue. This process, commonly executed through pyrolysis, plays a crucial role in determining the structural and functional properties of the resulting carbon materials [37]. Analyzing thermal degradation products helps to reveal both degradation and polymerization mechanisms [38–40]. Several studies have employed Fourier-transform infrared spectroscopy (FTIR) and gas chromatography–mass spectrometry (GC–MS) to investigate the breakdown of Mannich bases and the formation of benzoxazine dimers in different types of benzoxazines, including aromatic and aliphatic amine-based variations. Regardless of the type of phenolic linkage, the initial degradation products remain similar [41–44]. Low and Ishida identified ammonia as a key degradation product in aliphatic amine-based benzoxazines, whereas aniline-based benzoxazines exhibited minimal aromatic amine evaporation, due to stabilization by polymerized 3-aminophenylacetylene. Research indicates that NH-substituted benzoxazines, aniline, and unsaturated hydrocarbons emerge as degradation products following Mannich base cleavage, with the pathway influenced by temperature [45–48]. Another study found that non-aliphatic amine-based benzoxazines release p-aminotoluene at high temperatures, suggesting that benzoxazines with multiple dangling groups, particularly aliphatic amine variants, have lower thermal stability (Figure 4) [49].

Mannich base cleavage leads to two primary degradation pathways, which depend on whether the nitrogen is hydrogen-bonded. Hemvichan et al. [50] observed competition between C–C and C–N bond cleavage, with smaller amine linkages favoring C–C cleavage and bulkier ones preferring C–N cleavage. Modifying p-cresol-based benzoxazines with benzoyl chloride resulted in ester and secondary amine degradation products instead of primary amines, indicating that C–O bond cleavage may also occur due to resonance stabilization [51–53]. Hemvichan and Ishida further studied steric effects on bond cleavage in PH-a, BA-a, and BA-35x benzoxazines, synthesized from phenol, bisphenol A, and 3,5-xylidine. They found that C–C cleavage caused deaminomethylation, while C–N cleavage led to deamination, influenced by the nitrogen R-group. Radicals generated during degradation can recombine into dimers. In 2,4-dimethylphenol-based benzoxazines, C–C bond cleavage regenerates benzoxazine monomers, whereas C–N cleavage forms 2,4,6-trimethylphenols, which polymerize into bisphenol compounds. Similarly, biphenyls arise from phenolic radicals in p-cresol-based benzoxazines. Hemvichan and Ishida pro-

posed an alternative biphenyl formation mechanism, as mass spectrometry analysis of polybenzoxazine networks showed no secondary decomposition products [50].

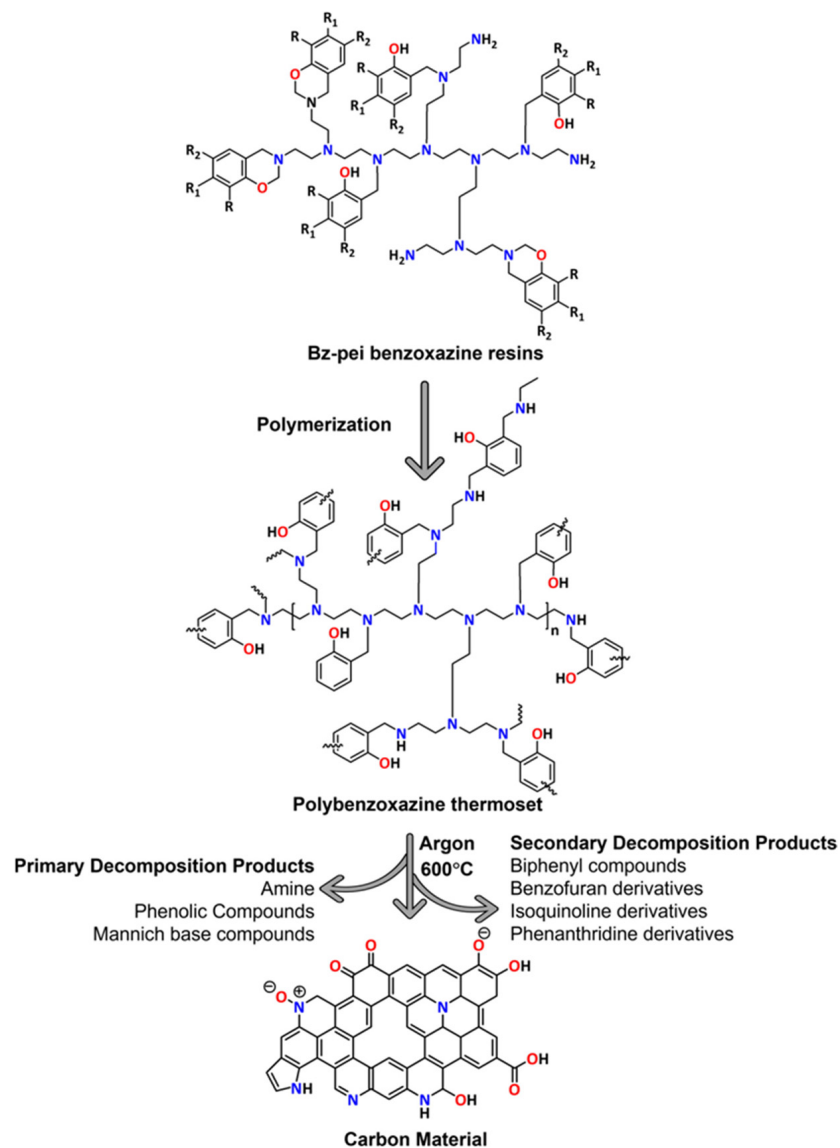


**Figure 4.** Carbonization process of nitrogen-enriched polybenzoxazine thermosets, specifically poly(G-pei(8:1)), poly(G-pei(10:1)), where R is  $-\text{OCH}_3$ , R1 is H, and R2 is H, and poly(C-pei(8:1)), poly(C-pei(10:1)), with R as H, R1 as  $\text{C}_{15}\text{H}_{31}$ , and R2 as H. Additionally, structure of nitrogen-doped carbon material is depicted, highlighting potential chemical states of heteroatoms within carbon framework [38].

### 3.2. Cross-Linking and Char Formation

The degree of cross-linking before and after thermal degradation plays a crucial role in char formation. Since char results from highly cross-linked structures, thermogravimetric analysis (TGA) has been widely used to explore degradation mechanisms involving cross-linking. Low and Ishida [44] examined acetylene-functionalized benzoxazines synthesized from 3-aminophenylacetate, paraformaldehyde, and various phenolic units (e.g., synthesized from polybenzoxazine colloidal spheres) using a template-free extended sol-gel approach, shown in Figure 5. They found that all the synthesized benzoxazines exhibited similar weight loss onset temperatures, indicating that cross-linking enhances carbonization, regardless of the phenolic linkage. TGA data also suggested that phenol and bisphenol contribute to cross-linking, explaining why benzoxazines based on p-cresol had lower char

yields than those derived from 2,4-dimethylphenol and modified p-cresol. Bagherifam et al. [54] observed that poly(PH-ma) benzoxazines, where cross-linking occurs via -NCH<sub>2</sub> groups in the oxazine ring, exhibited increased post-degradation cross-linking after side-chain loss. Similarly, benzoxazines with sulfur linkages demonstrated strong char-forming potential. Liu et al. [47] synthesized bisphenol-S-based benzoxazines and analyzed them using thermogravimetric mass spectrometry (TG-MS). They identified early-stage Schiff base cleavage, followed by sulfurous gas release at 330 °C due to C–S bond scission, leading to more carbocation fragments at elevated temperatures. Further studies on PBS-m benzoxazines revealed that weaker C–H and C–N bonds in methylamine increased carbon and hydrogen evolution during degradation. Hamerton et al. [52] confirmed that the lower dissociation energy of C–N bonds in sulfur-linked benzoxazines made them more susceptible to thermal cleavage. Zhu et al. [42] explored nitro-substituted benzoxazines, and found that the electron-withdrawing nitro group weakened aromatic ring stability, increasing weight loss. Despite this, the resulting char remained chemically stable under various conditions.

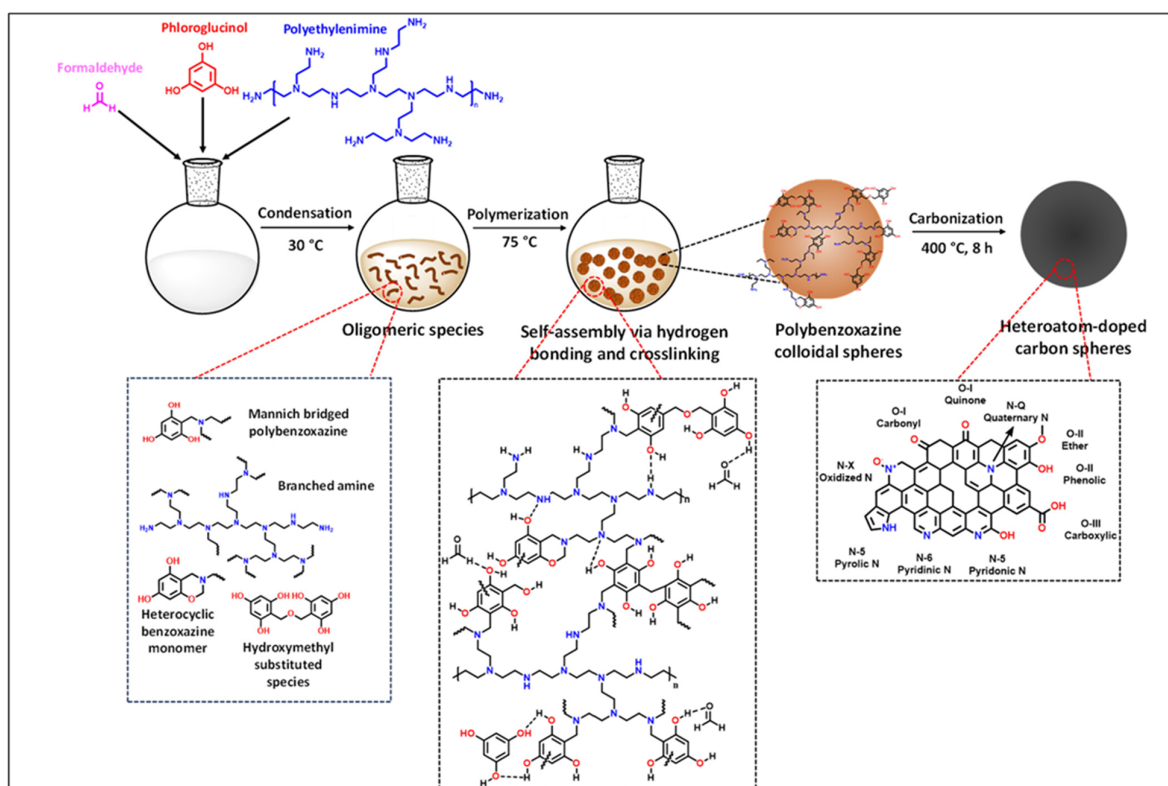


**Figure 5.** Schematic representation of N, O-co-doped carbon particles synthesized from polybenzoxazine colloidal spheres using template-free extended sol-gel approach [37].

#### 4. Polybenzoxazine-Based Carbons and Their Electrochemical Performance

##### 4.1. Autocatalysis Synthesis of Poly(benzoxazine-co-resol)-Based Polymer and Carbon Spheres

Zhao et al. (2018) [55] introduced an innovative approach to synthesize highly monodisperse poly(benzoxazine-co-resol)-based polymer and carbon spheres via autocatalysis polymerization of 3-aminophenol and formaldehyde. Unlike conventional methods that require external catalysts, surfactants, or templates, this study demonstrated that 3-aminophenol itself acts as both a reactant and a catalyst, due to its unique molecular structure. The polymerization process was studied extensively using Fourier-transform infrared (FTIR), nuclear magnetic resonance (NMR), and X-ray photoelectron spectroscopy (XPS)

techniques. The researchers found that the polymer spheres could be precisely tuned in size from 372 to 1030 nm by varying the reaction temperature and monomer concentrations.

These polymer spheres exhibited excellent thermal stability, enabling their transformation into nitrogen-doped carbon spheres via carbonization (Figure 6). The electrochemical performance of the carbon spheres was investigated to assess their potential application in energy storage. The authors highlighted that the nitrogen doping from 3-aminophenol enhanced the conductivity and electrochemical activity of the resulting carbon material. The obtained carbon spheres retained a well-defined structure (Figure 7), contributing to high capacitance and excellent cycling stability when used in supercapacitor applications [55–57]. Electrochemical tests were carried out to evaluate the charge storage capabilities of the synthesized carbon spheres. The results indicated that these materials exhibited superior electrochemical properties, due to their highly porous nature and nitrogen doping. The nitrogen-doped carbon spheres showed promising energy storage characteristics, making them potential candidates for applications such as supercapacitors and batteries. The study emphasized that this low-cost, environmentally friendly, and scalable method could be highly beneficial for industrial production and further energy storage advancements.

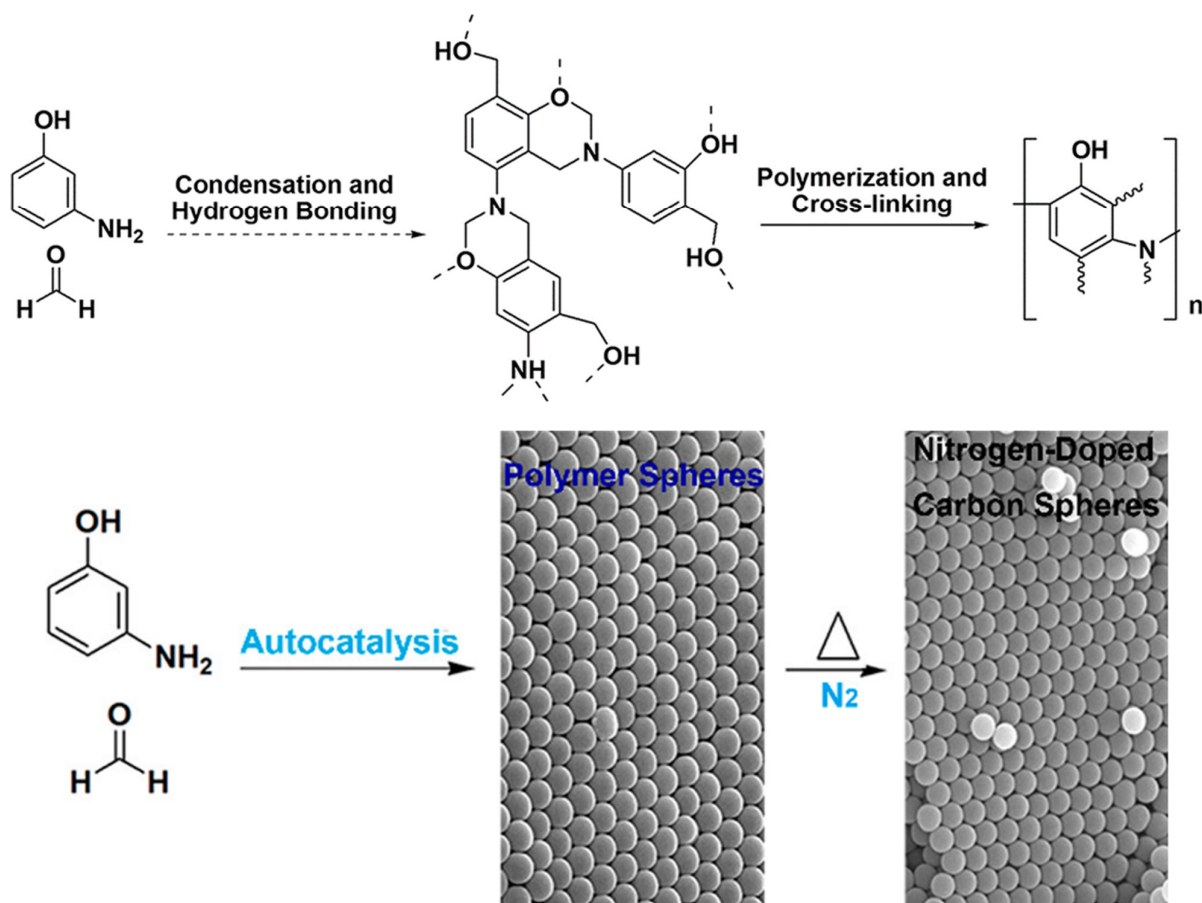


**Figure 6.** Synthesis process of highly monodisperse resin polymer spheres and nitrogen-doped carbon spheres using 3-aminophenol and formaldehyde as monomers [55].

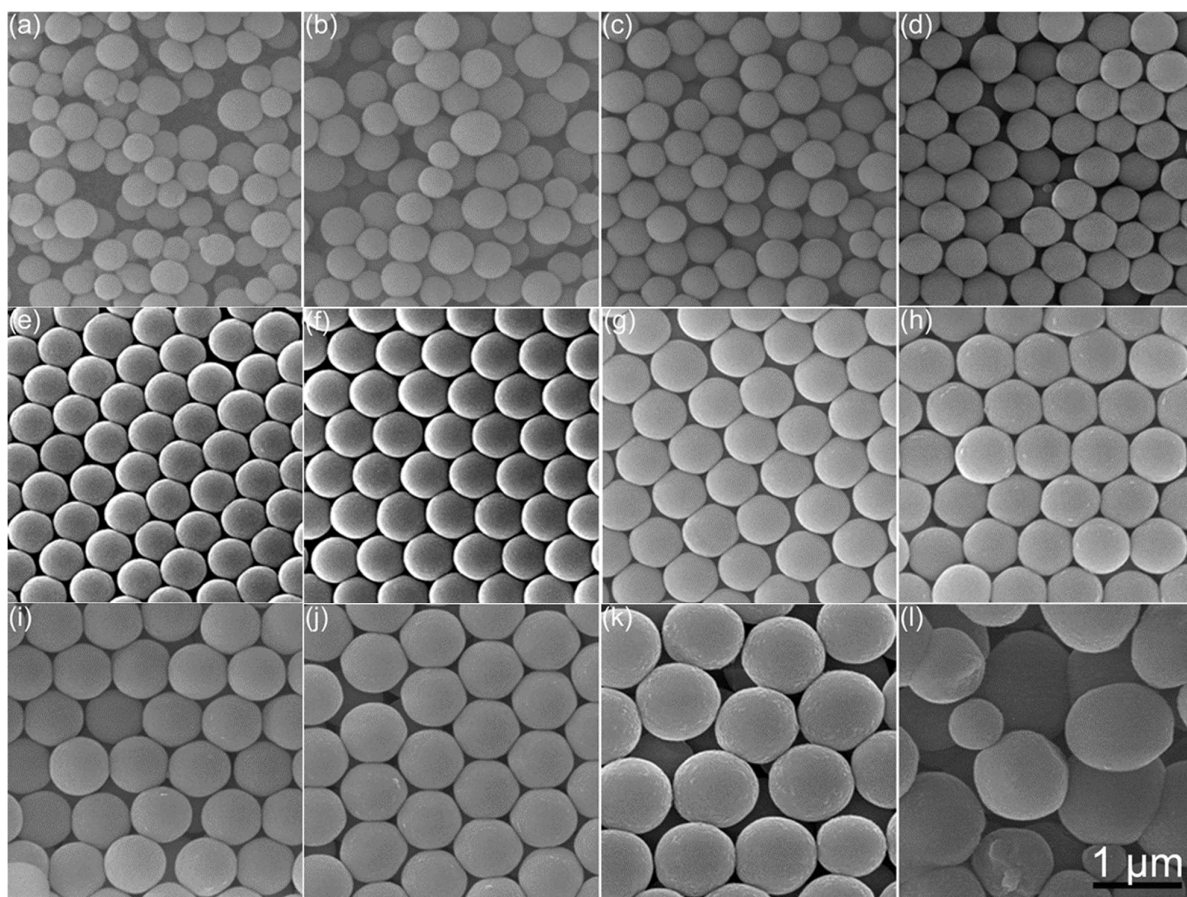


**Figure 7.** SEM images (a–l) of APFS synthesized with varying 3-aminophenol concentrations: (a) 5 mmol/L (APFS-9), (b) 7.5 mmol/L (APFS-10), (c) 10 mmol/L (APFS-11), (d) 15 mmol/L (APFS-12), (e) 20 mmol/L (APFS-13), (f) 25 mmol/L (APFS-14), (g) 30 mmol/L (APFS-15), (h) 50 mmol/L (APFS-16), (i) 60 mmol/L (APFS-17), (j) 80 mmol/L (APFS-18), (k) 160 mmol/L (APFS-19), and (l) 320 mmol/L (APFS-20). The scale for (a–k) matches that of (l) [55].

#### 4.2. Template-Free, Self-Doped Approach to Porous Carbon Spheres for High-Performance Supercapacitors

Xue et al. (2019) [58] developed a novel method for fabricating nitrogen- and oxygen-enriched porous carbon spheres (PCSs) using a template-free and self-doping approach, as shown in Figure 8. The method involved the direct carbonization and activation of melamine-glyoxal polymer, leading to interconnected carbon spheres with a high nitrogen and oxygen content. The study highlighted that the interconnected spherical morphology provided ion reservoirs for rapid ion diffusion and facilitated electron transport through conductive networks. The synthesized PCSs exhibited a large surface area ( $1302 \text{ m}^2/\text{g}$ ) and an optimized hierarchical pore structure that significantly enhanced their electrochemical performance.

The authors systematically evaluated the electrochemical properties of PCSs for supercapacitor applications, as represented in Figure 9a–g. The synthesized materials showed high specific capacitance values of up to  $344 \text{ F/g}$  at  $1.0 \text{ A/g}$ , coupled with excellent rate capability and long-term cycling stability. The high N/O content improved surface wettability, allowing better contact with electrolytes and contributing to additional pseudocapacitance through redox reactions. Furthermore, the researchers assembled symmetric supercapacitors using PCS electrodes, achieving an impressive energy density of  $33.37 \text{ Wh/kg}$  with a power density of  $9000 \text{ W/kg}$  in  $\text{Na}_2\text{SO}_4$  electrolyte.

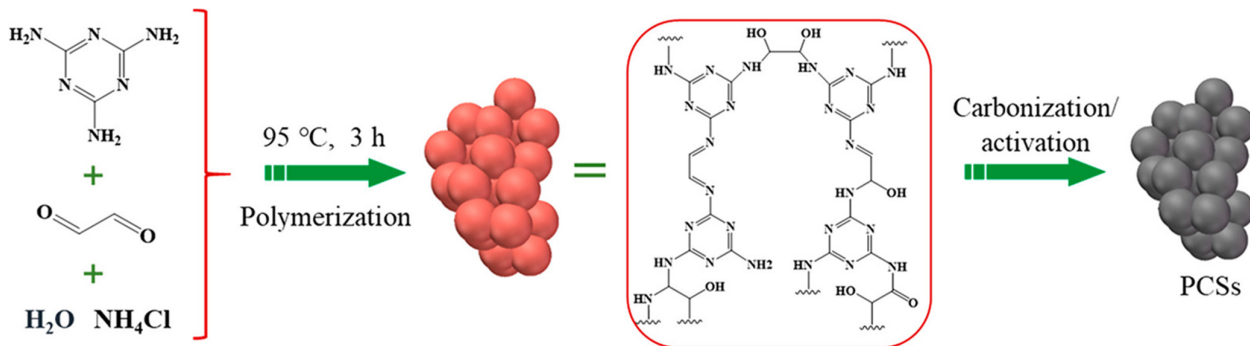


**Figure 8.** Schematic illustration of PCS synthesis via melamine/glyoxal polymerization followed by single-step carbonization and activation process [58].

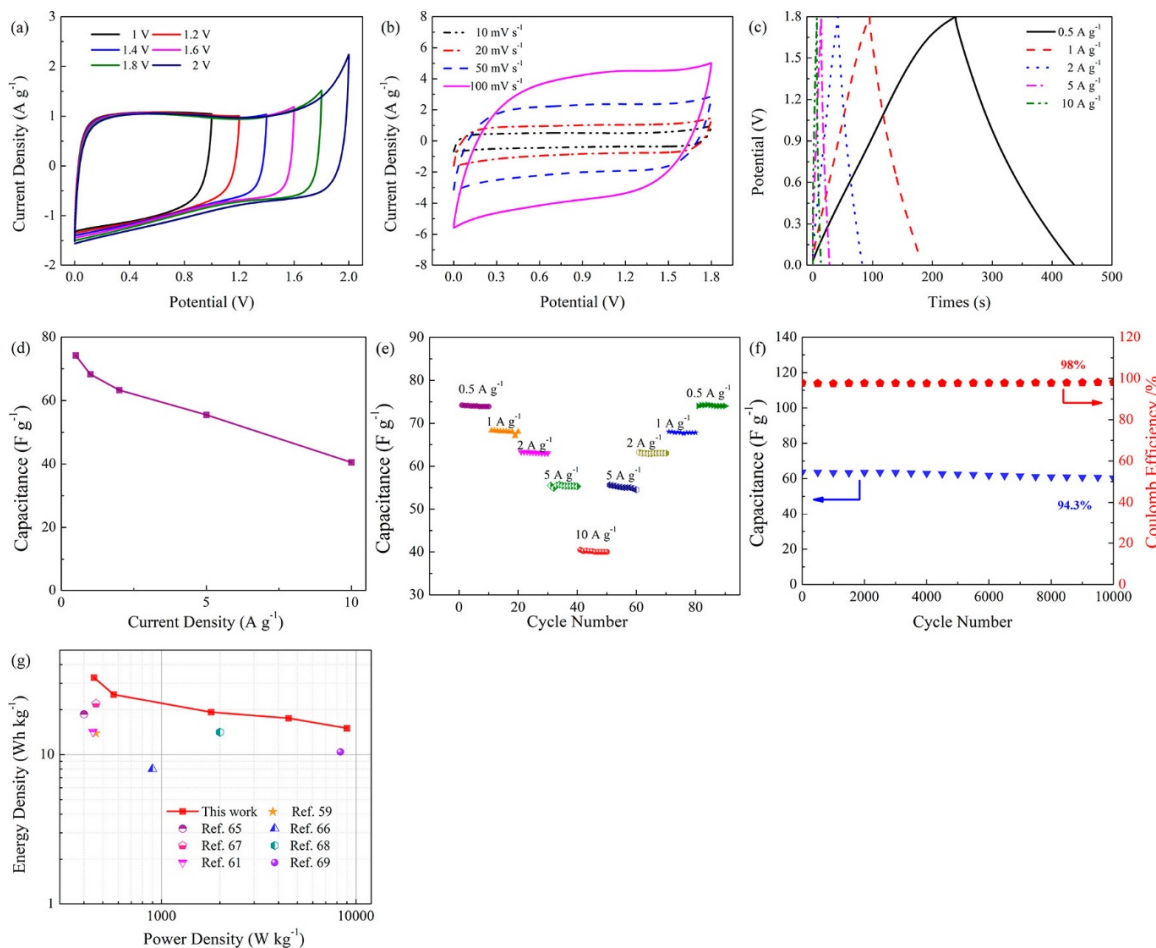


**Figure 9.** Electrochemical performance of PCS800-based symmetric supercapacitor using  $\text{Na}_2\text{SO}_4$  solution: (a) CV curves across different potential windows at scan rate of  $10 \text{ mV s}^{-1}$ , (b) CV curves at varying scan rates, (c) GCD curves at different current densities, (d) specific capacitance values at various current densities, (e) rate performance of device, (f) cycling stability and Coulombic efficiency at  $2.0 \text{ A g}^{-1}$  over 10,000 cycles, and (g) Ragone plots comparing device with recently reported carbon-based supercapacitors [58].

The study underscored the importance of controlling pore size and doping levels to optimize electrochemical performance. The presence of micro-, meso-, and ultra-micropores in the PCSs played a crucial role in enhancing charge storage and ion diffusion. Compared to traditional template-assisted methods, this self-doped strategy not only simplified the fabrication process, but also resulted in highly efficient carbon materials with superior electrochemical performance [58]. The findings suggest that these PCSs could be widely

used in energy storage applications, offering a sustainable alternative for high-performance supercapacitors.

#### 4.3. Supermolecule Self-Assembly Promotes Porous N, P Co-Doped Reduced Graphene Oxide for High-Energy Supercapacitors

Cheng et al. (2019) [59] introduced an innovative supramolecular self-assembly method to synthesize nitrogen- and phosphorus-co-doped reduced graphene oxide (NP-rGO) for high-energy supercapacitor applications. The study leveraged a combination of graphene oxide (GO), melamine, and phytic acid to create a supramolecular polymer system, which, upon heat treatment, resulted in a three-dimensional (3D) porous graphene structure. The NP-rGO material exhibited a loose-packed, crumpled, thin-layer morphology, which significantly improved its electrochemical properties (Figure 10). The presence of nitrogen and phosphorus in the graphene framework enhanced both the conductivity and the pseudocapacitance, making it a promising electrode material.

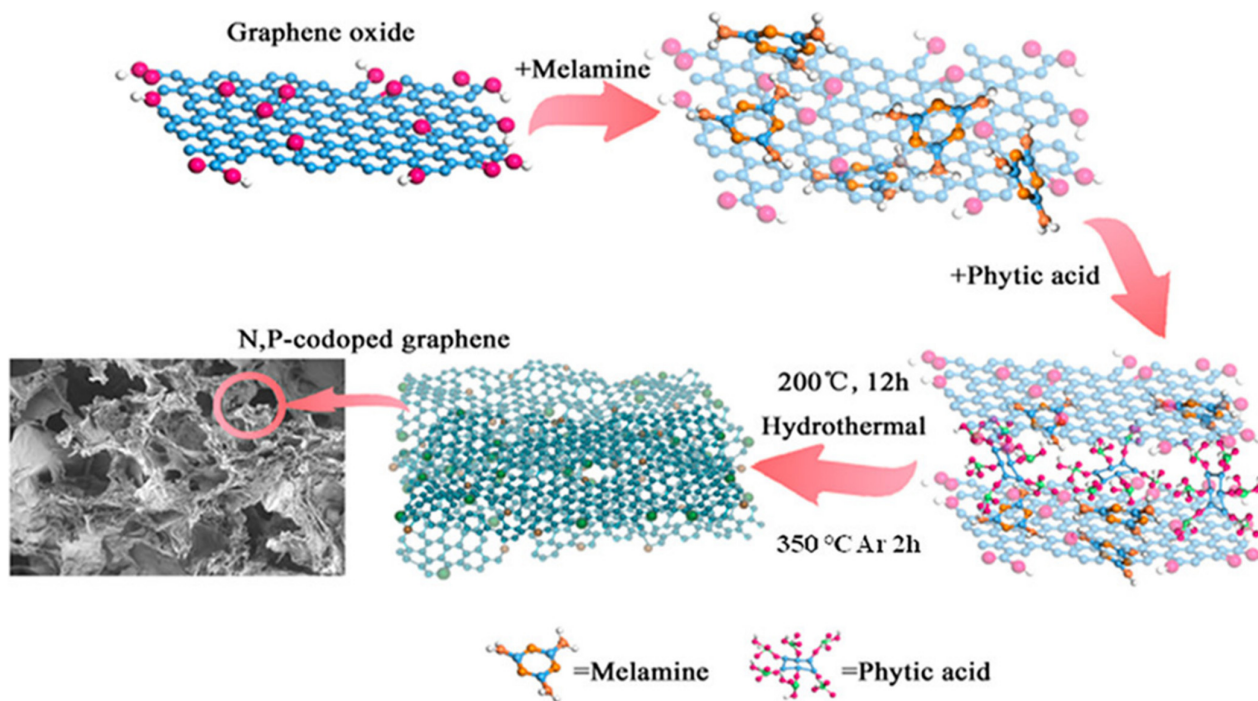


**Figure 10.** Schematic representation of NP-rGO material synthesis via supramolecular polymerization [59].

The electrochemical evaluation of NP-rGO, as shown in Figure 11a–f, demonstrated its superior capacitive properties compared to undoped graphene. The NP-rGO exhibited a high specific capacitance of 416 F/g, and maintained 94.63% capacitance retention after 10,000 cycles, confirming its excellent cycling stability. Moreover, the study revealed that the synergistic effect of N and P doping contributed to enhanced charge storage through pseudocapacitive mechanisms. The material's porous structure facilitated rapid ion diffusion and minimized resistance, further boosting its energy storage performance [59,60].

In addition to supercapacitor electrodes, NP-rGO was tested in symmetric supercapacitors, where it delivered an energy density of 22.3 Wh/kg at a power density of 500 W/kg. The superior performance was attributed to the tailored 3D porous morphology and the strategic co-doping of nitrogen and phosphorus, which introduced additional active sites for electrochemical reactions. The study concluded that the supramolecular self-assembly approach could serve as a scalable and cost-effective method for producing

high-performance graphene-based materials, with significant potential in next-generation energy storage devices.

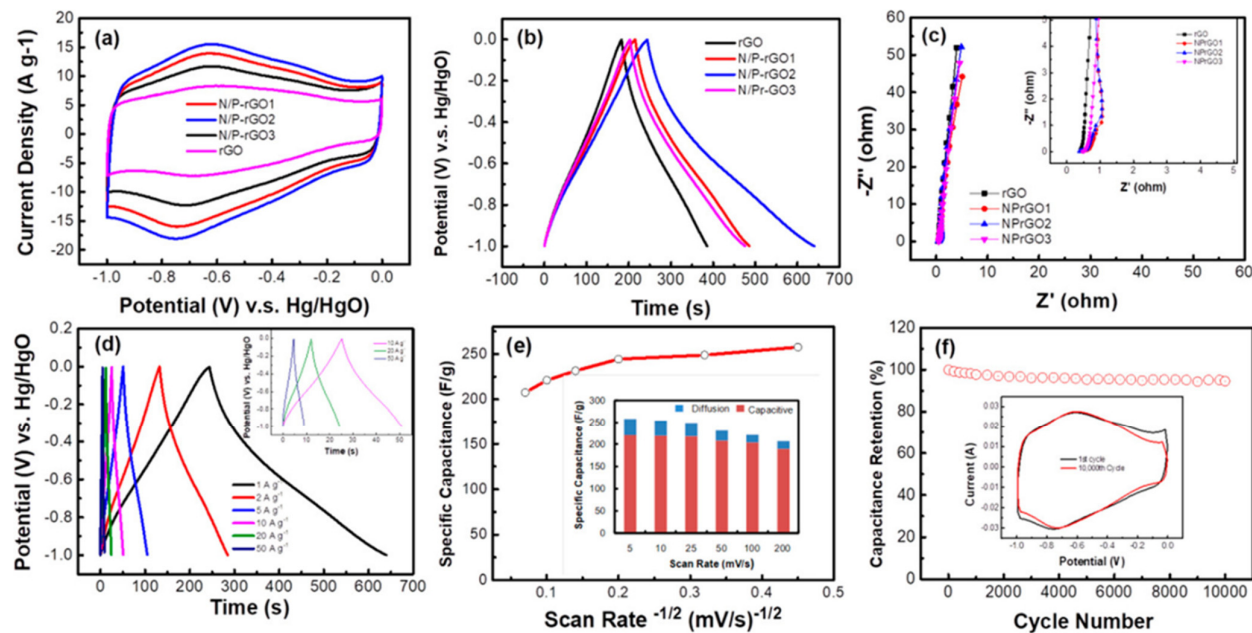


**Figure 11.** (a) CV curves of rGO and NP-rGO<sub>x</sub> ( $x = 1, 2, 3$ ) at  $5 \text{ mV s}^{-1}$ . (b) GCD curves of rGO and NP-rGO<sub>x</sub> ( $x = 1, 2, 3$ ) at  $1 \text{ A g}^{-1}$ . (c) Nyquist plots (0.01 Hz–100 kHz) at open circuit potential. (d) GCD curves of NP-rGO<sub>2</sub> from 1 to  $50 \text{ A g}^{-1}$ . (e) Infinite scan rate capacitance of NP-rGO<sub>2</sub> (inset: diffusion vs. capacitive contributions). (f) Cycling stability of NP-rGO<sub>2</sub> at  $100 \text{ mV s}^{-1}$ . All tests conducted in 6 M KOH [59].

#### 4.4. Electrochemical Aspects of Cross-Linked Polybenzoxazole Aerogels

The study by Ma et al. (2021) [61] focuses on developing cross-linked polybenzoxazole (cPBO) aerogels from polybenzoxazine (Figure 12a,b), primarily emphasizing their structural, thermal, and mechanical properties. These aerogels exhibit excellent thermal stability, fire resistance, and low dielectric properties, making them promising materials for various advanced applications. While the research does not explicitly investigate electrochemical properties, the inherent characteristics of these aerogels suggest their potential utility in energy storage systems.

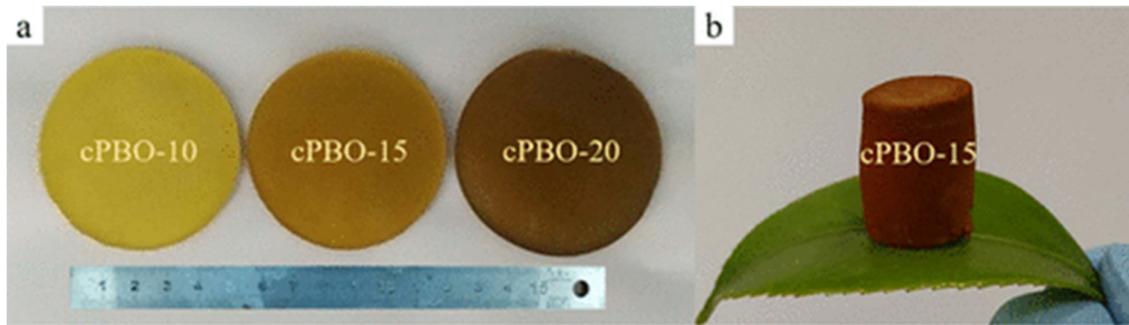


**Figure 12.** Digital images of cPBO aerogels [61].

The porous structure of the cPBO aerogels, shown in Figure 13a–f, provides a high surface area, which is a critical factor in electrochemical applications. The electronic transmission properties of PBO indicate that these materials could serve as electrode components in capacitors or batteries. Their high mechanical strength ensures durability under repeated charge–discharge cycles, a crucial requirement for electrochemical devices.

Although direct electrochemical testing is absent from this study, the aerogels' structural stability and retained porosity after heat treatment imply their suitability for applications that demand high conductivity and low dielectric loss. Future research could incorporate dopants or conductive fillers to further explore the electrochemical potential of these materials in supercapacitor or battery electrodes [61,62].

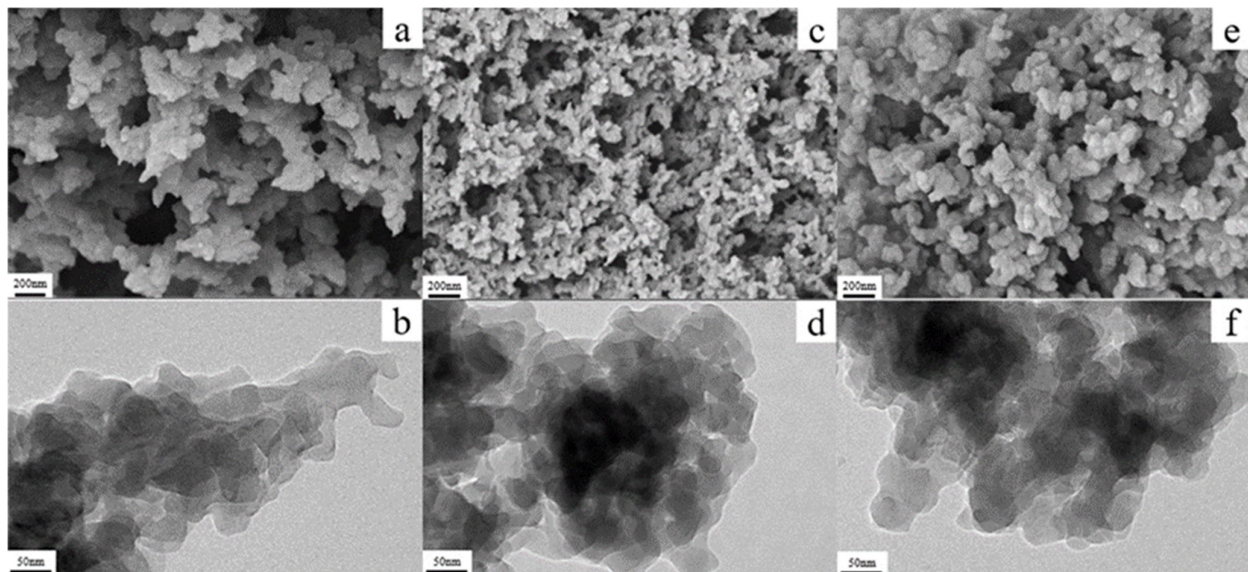


**Figure 13.** SEM and TEM images of cPBO-10 (a,b), cPBO-15 (c,d), and cPBO-20 (e,f) aerogels [61].

Despite the lack of electrochemical testing, the intrinsic properties of these aerogels suggest their possible applications in energy storage devices. Their low dielectric constant could make them effective in improving charge retention and reducing leakage currents in capacitors. Their stability under thermal stress also indicates their potential use in high-temperature energy storage environments. Further modification of these materials through nitrogen doping or hybridization with conductive nanomaterials could significantly enhance their electrochemical activity. Given their structural robustness, these aerogels could be integrated into composite electrodes for supercapacitors, where the combination of porosity and stability would provide high energy and power densities [63].

#### 4.5. Electrochemical Aspects of Nitrogen-Rich Porous Carbon/NiMn Hybrids for Supercapacitors

Periyasamy et al. (2022) [64] explore the electrochemical potential of nitrogen-rich porous carbon (NRPC) hybrids embedded with nickel and manganese (NiMn) for supercapacitor electrodes. The primary focus of this study is to enhance charge storage capability through a combination of electric double-layer capacitance and pseudocapacitive effects. The nitrogen-doped carbon framework (Figure 14) improves conductivity and wettability, while the transition metal components contribute redox-active sites that enhance Faradaic charge storage.

Cyclic voltammetry (CV) studies reveal a combination of EDLC and pseudocapacitance, indicating that the NRPC/NiMn electrodes can efficiently store charge through both electrostatic adsorption and reversible redox reactions, as shown in Figure 15a–d. The CV profiles show broad redox peaks, suggesting a strong contribution of transition metal oxides to capacitance enhancement. The NRPC/NiMn hybrid exhibits a high specific capacitance of 1825 F/g, significantly outperforming pure NRPC and single-metal hybrids, demonstrating the synergistic effect of bimetallic incorporation.

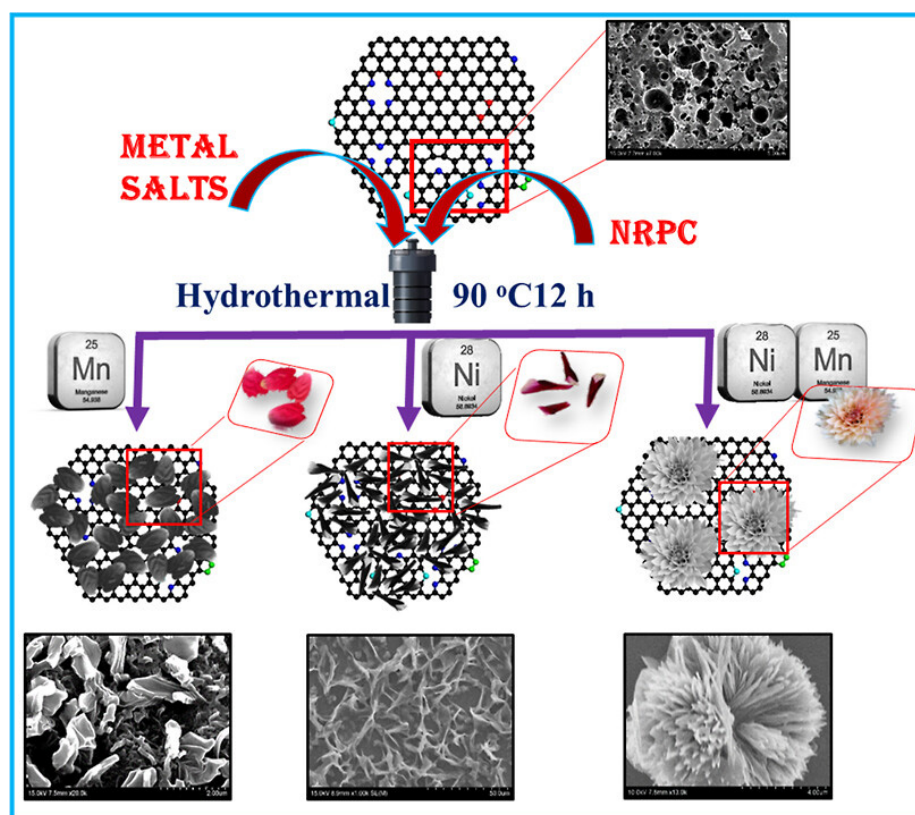


**Figure 14.** Diagram depicting synthesis and structure of NRPC/Mn, NRPC/Ni, and NRPC/NiMn [64].

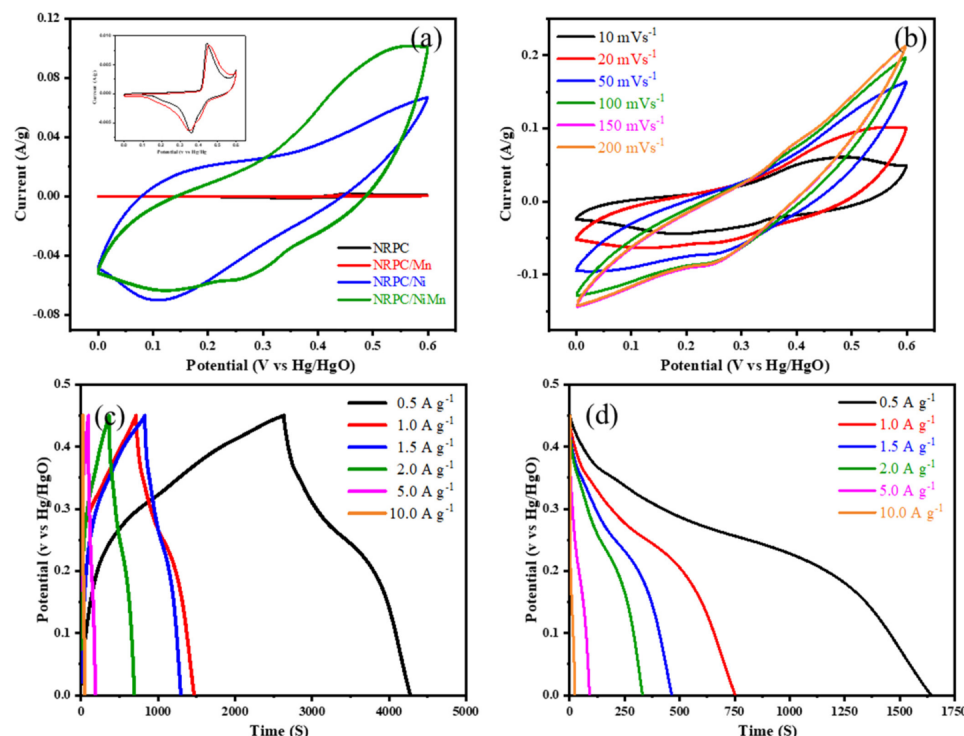


**Figure 15.** (a) Cyclic voltammetry (CV) profiles of synthesized samples at 20 mV/s; (b) CV profiles for NRPC/NiMn; (c) galvanostatic charge–discharge (GCD) curves of NRPC/NiMn; and (d) discharge profiles of NRPC/NiMn [64].

Galvanostatic charge–discharge (GCD) tests confirm the high energy storage efficiency of NRPC/NiMn, with a retention of 78% capacitance after 2500 cycles. The stability of the

electrodes under prolonged cycling highlights the robust nature of the hybrid material. The 3D flowerlike morphology observed in SEM imaging further supports the material's superior electrochemical performance, as it enhances electrolyte penetration and facilitates efficient ion transport. The hierarchical porous network reduces internal resistance and improves the accessibility of electroactive sites, leading to improved charge storage dynamics [64,65]. Electrochemical impedance spectroscopy (EIS) measurements confirm the low charge transfer resistance of NRPC/NiMn, emphasizing its excellent conductivity and rapid electron transport capabilities. Compared to traditional carbon-based supercapacitors, which primarily rely on EDLC, the presence of transition metal oxides allows for additional Faradaic reactions that significantly boost capacitance. These findings suggest that NRPC/NiMn hybrids are promising candidates for next-generation energy storage devices, particularly in high-power applications requiring rapid charge–discharge cycles. The charge–discharge efficiency and Coulombic efficiency of these electrodes indicate minimal energy losses during cycling, making them viable for commercial applications. Compared to commercial activated carbon electrodes, the NRPC/NiMn system exhibits nearly double the capacitance, making it a strong contender for integration into hybrid supercapacitor–battery systems. Future work could involve optimizing the metal-to-carbon ratio to maximize both energy and power density while maintaining long-term stability [64,66].

#### 4.6. Electrochemical Aspects Upcycling Polybenzoxazine Thermosets into N-Doped Carbon for Supercapacitors

Sharma et al. (2023) [67] focus on the sustainable upcycling of nitrogen-enriched polybenzoxazine thermosets into nitrogen-doped carbon materials, aiming to produce high-performance supercapacitor electrodes. This study emphasizes the role of nitrogen doping in enhancing the electrochemical properties of the derived carbon, particularly in terms of pseudocapacitive behavior and improved conductivity (Figure 16).

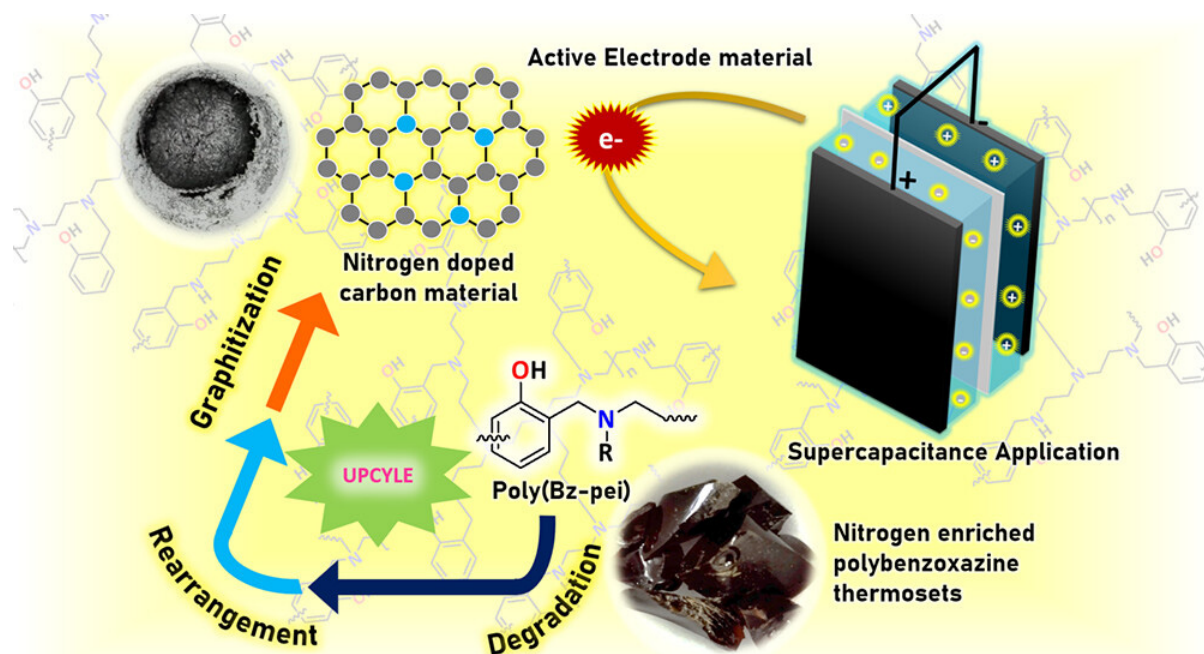


**Figure 16.** Diagram illustrating transformation of nitrogen-enriched polybenzoxazine thermosets into nitrogen-doped carbon materials for development of high-performance supercapacitors [67].

Cyclic voltammetry results for the nitrogen-doped carbon electrodes show well-defined redox peaks, indicating significant Faradaic contribution, alongside EDLC behavior

(Figure 17a–f). The best-performing electrode, labeled C-GP81, achieves an exceptional capacitance of 700 F/g at 10 A/g. This high value surpasses many previously reported polybenzoxazine-derived carbons, suggesting that the nitrogen doping strategy effectively enhances charge storage capabilities. The presence of graphitic nitrogen and pyrrolic nitrogen species improves electronic conductivity and facilitates charge transfer during redox reactions [67,68]. Galvanostatic charge–discharge tests confirm the electrode’s high energy density of 48 Wh/kg at a power density of 8400 W/kg, positioning it among the top-performing carbon-based supercapacitors. This indicates that the nitrogen-doped carbon framework is not only capable of storing large amounts of charge, but can also deliver energy at high rates, making it suitable for applications requiring rapid energy delivery, such as in regenerative braking systems and portable electronic devices.

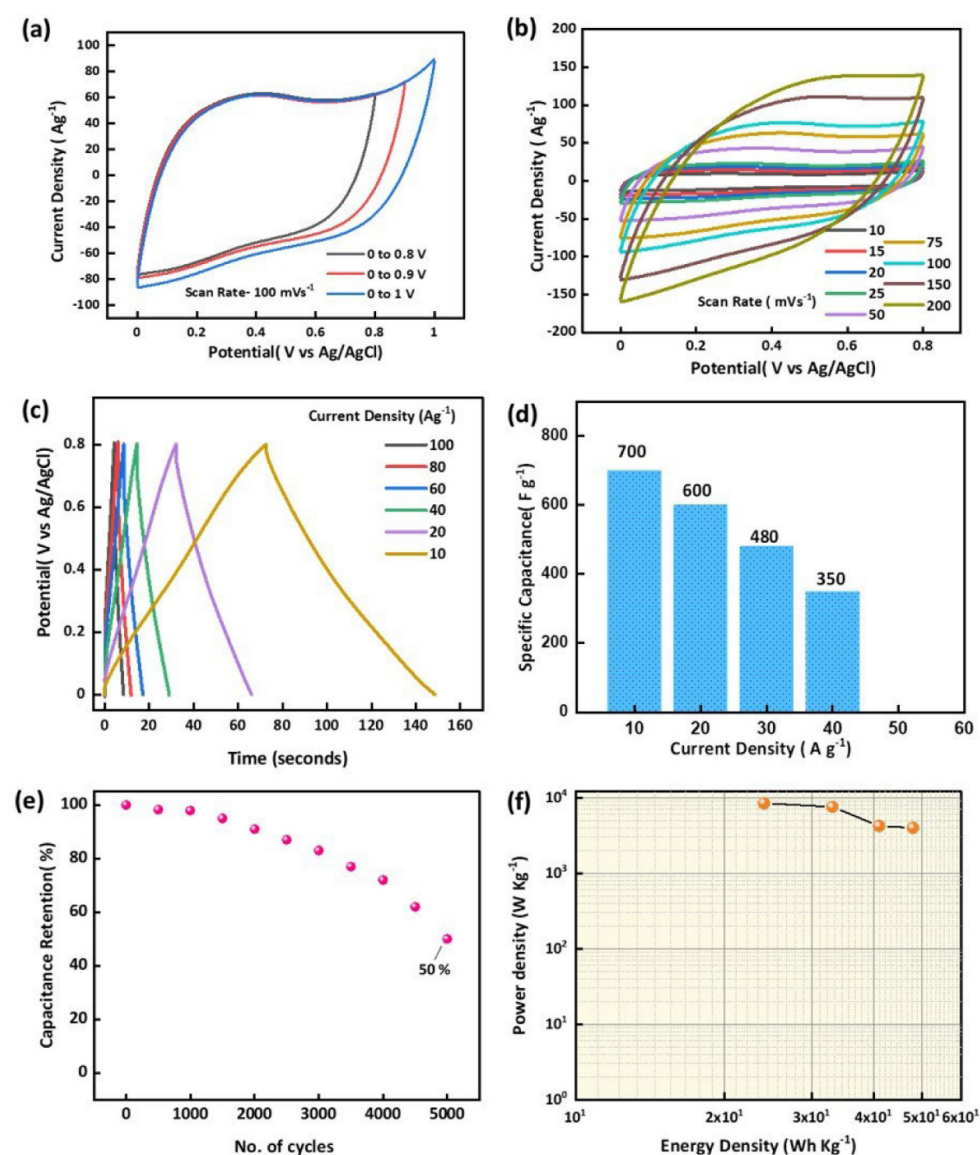


**Figure 17.** Electrochemical behavior (measured using three-electrode setup) of carbon material C-GP81 on carbon cloth as active material. (a) CV curves at scan rate of  $100 \text{ mV s}^{-1}$  across various potential windows, (b) CV curves at selected potential window with different scan rates, (c) GCD profiles at varying current densities, (d) change in specific capacitance with respect to current density, (e) stability of supercapacitive performance over 5000 cycles, and (f) Ragone plot comparing energy density and power density [67].

Electrochemical impedance spectroscopy measurements further support these findings, with the nitrogen-doped carbon material displaying low equivalent series resistance (ESR) and high ion mobility within the electrolyte. The hierarchical porosity of the carbon structure ensures rapid ion diffusion, enabling efficient charge–discharge cycles. Additionally, long-term cycling stability tests demonstrate outstanding performance retention, with the electrodes maintaining nearly 90% of their initial capacitance, even after 10,000 cycles. The superior electrochemical performance of these nitrogen-doped carbons can be attributed to their tailored porous structure, optimized surface chemistry, and high nitrogen content. Unlike conventional carbon materials, which often require harsh chemical activation steps, the upcycled nitrogen-doped carbons in this study achieve high electrochemical activity through a sustainable and cost-effective approach. The researchers suggest that future optimizations, such as hybridizing these carbons with metal oxides or incorporating additional heteroatom dopants, could further elevate their energy storage capabilities [67–69].

#### 4.7. Electrochemical Aspects of Enhanced Electrochemical Performance of HC/NiCo@800C Using Redox-Active Electrolytes

The study by Asrafali et al. (2024) [70] presents a significant advancement in the field of supercapacitors by developing a hybrid energy storage system combining electrical double-layer capacitance (EDLC) and pseudocapacitance. The research explores the synergistic effects of heteroatom-doped carbon (HC) and bimetallic NiCo oxide ( $\text{NiCo}_2\text{O}_4$ ) in the presence of redox-active electrolytes containing iodide ions ( $\text{KI}$  and  $\text{RbI}$ ) (Figure 18). This approach leads to a considerable enhancement in electrochemical performance, specifically in energy density and capacitance retention.

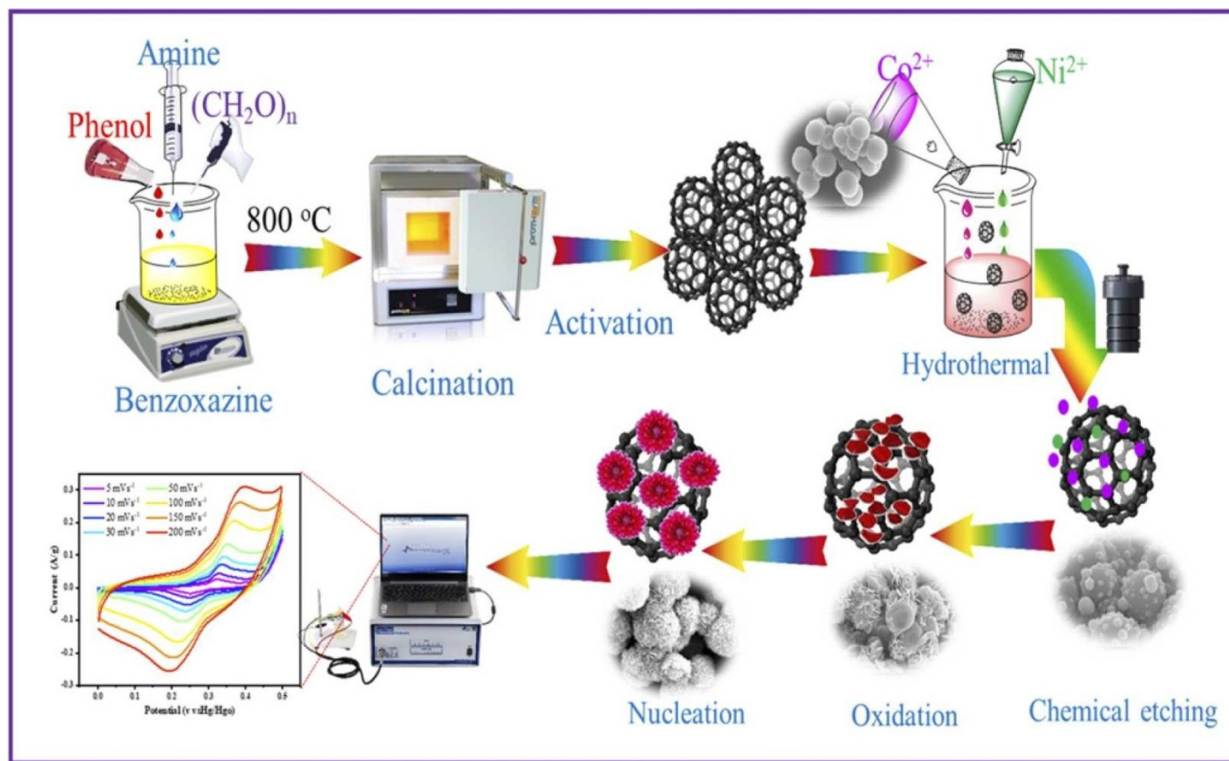


**Figure 18.** Diagram illustrating formation of HC/NiCo at 800 °C [70].

CV results demonstrate the material's ability to facilitate both EDLC and pseudocapacitive charge storage, as evidenced by well-defined redox peaks in the presence of iodide-based electrolytes (Figure 19a–f). The introduction of redox-active species further

amplifies capacitance by promoting additional Faradaic reactions. The specific capacitance values recorded are remarkable, reaching  $2334 \text{ F g}^{-1}$  at  $1 \text{ A g}^{-1}$  for RbI and  $2076 \text{ F g}^{-1}$  for KI. These values are significantly higher compared to conventional aqueous KOH electrolyte, emphasizing the role of redox-active electrolytes in enhancing charge storage capacity [70,71].

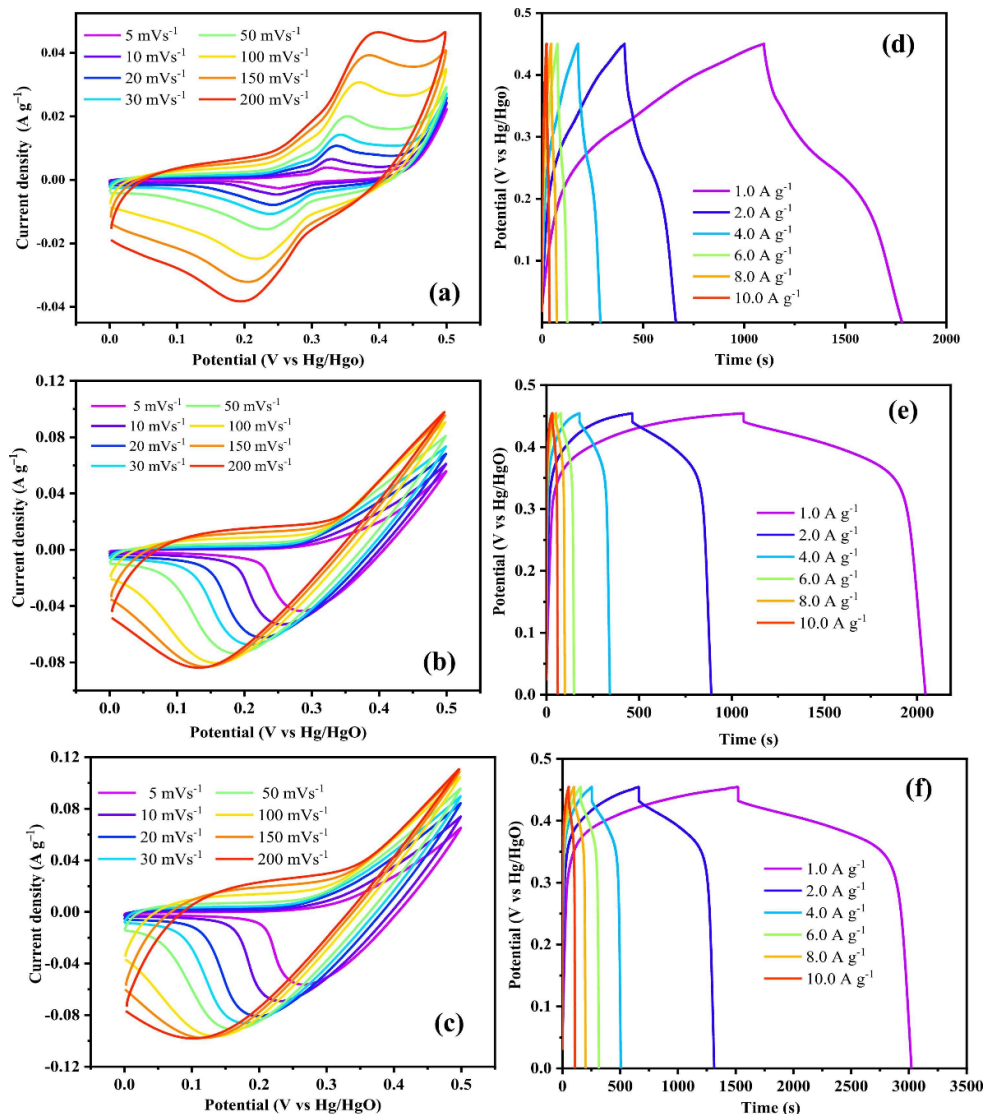


**Figure 19.** Electrochemical data from 3-electrode system, displaying CV and GCD curves of HC/NiCo@800C in 1 M KOH (a,d), 1 M KI (b,e), and 1 M RbI (c,f) [70].

GCD measurements confirm the high energy storage efficiency of the HC/NiCo@800C electrode. An asymmetric supercapacitor device (HC/NiCo@800C // HC) is fabricated, demonstrating a specific capacitance of  $232 \text{ F g}^{-1}$  and an increased energy density of  $96.57 \text{ W-h kg}^{-1}$  with RbI as the electrolyte. These results highlight the superior charge storage ability of the hybrid electrode, which maintains structural stability and high reversibility, even after prolonged cycling. EIS further supports these findings by revealing a low charge transfer resistance and enhanced conductivity, attributed to the bimetallic  $\text{NiCo}_2\text{O}_4$  phase and heteroatom doping in the carbon framework. The interconnected mesoporous structure of the material facilitates rapid ion diffusion, which is essential for maintaining high power density and efficient charge transfer. Overall, this study underscores the importance of utilizing both electrode material modifications and innovative electrolyte strategies to max-

imize supercapacitor performance, positioning the HC/NiCo@800C system as a promising candidate for next-generation energy storage applications [63,70].

#### 4.8. Electrochemical Aspects of Controllable Synthesis of Bifunctional Porous Carbon for Supercapacitors

Wang et al. (2018) [72] introduced a novel approach to synthesizing biomass-derived, nitrogen-doped porous carbon (NAPC) for use in supercapacitor electrodes. This work highlights the tunability of pore structure and surface chemistry to optimize electrochemical performance, particularly in aqueous KOH electrolyte (Figure 20a–e). The key innovation lies in the controlled activation of algae-derived carbon, which yields a high specific surface area of  $1538.7 \text{ m}^2 \text{ g}^{-1}$  and a well-balanced microporous/mesoporous architecture conducive to efficient charge storage.

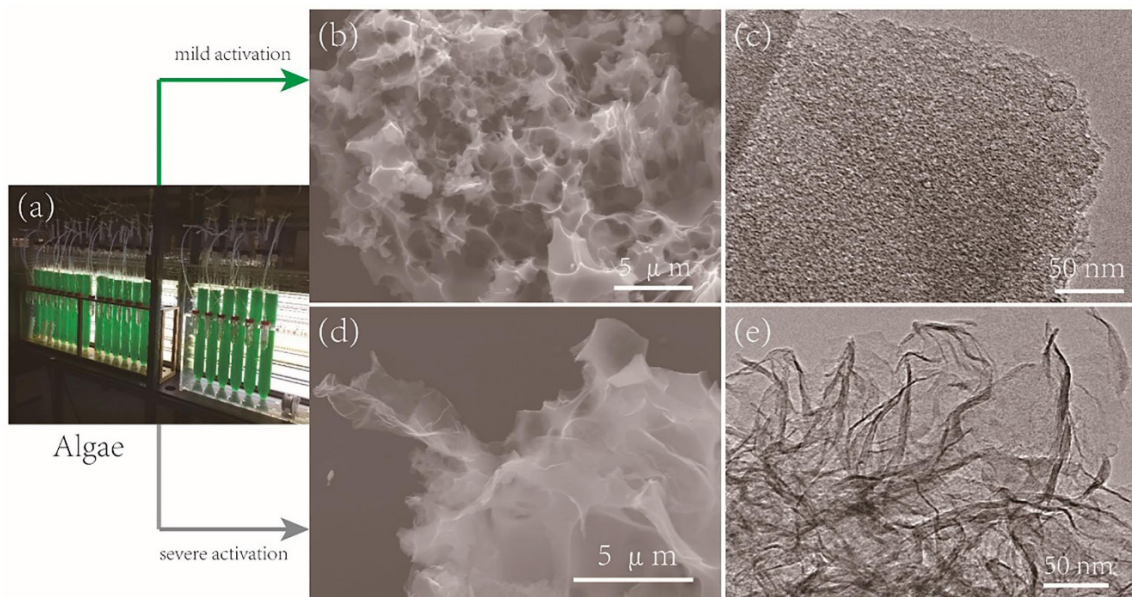


**Figure 20.** (a) Photo of algae cultivation system; SEM images of (b) NAPC-2-6 and (d) NAPC-2-9; TEM images of (c) NAPC-2-6 and (e) NAPC-2-9 [72].

Cyclic voltammetry analysis of NAPC electrodes exhibits quasi-rectangular profiles with minimal distortion, indicating an ideal EDLC behavior (Figure 21a–e). The incorporation of nitrogen heteroatoms enhances charge storage by introducing additional active sites for ion adsorption, thereby increasing capacitance. The specific capacitance values recorded are  $287.7 \text{ F g}^{-1}$  at  $0.2 \text{ A g}^{-1}$  in a three-electrode setup, and  $190.0 \text{ F g}^{-1}$  in a two-electrode system. Notably, the material retains 79.3% of its capacitance at a high current density of  $10 \text{ A g}^{-1}$ , showcasing excellent rate capability. Galvanostatic charge–discharge measurements further affirm the electrode’s outstanding performance, with a high cycling stability of 98% capacitance retention after 8000 cycles. This exceptional durability is attributed to the robust carbon framework and hierarchical porosity, which facilitate rapid ion diffusion and reduce internal resistance. Compared to conventional activated carbons, the NAPC material demonstrates superior electrochemical characteristics, particularly in long-term cycling and high-rate operations [72,73]. Electrochemical impedance spectroscopy results confirm the low equivalent series resistance (ESR) of the material, indicating efficient charge transfer dynamics. The well-defined pore structure allows for effective electrolyte penetration, further improving charge storage efficiency. Given these advantages, the algae-derived NAPC emerges as a cost-effective and environmentally sustainable alternative to traditional carbon-based supercapacitor electrodes. The study suggests future directions

in optimizing heteroatom doping strategies and hybridizing NAPC with metal oxides to further enhance its electrochemical properties [69,71,72].

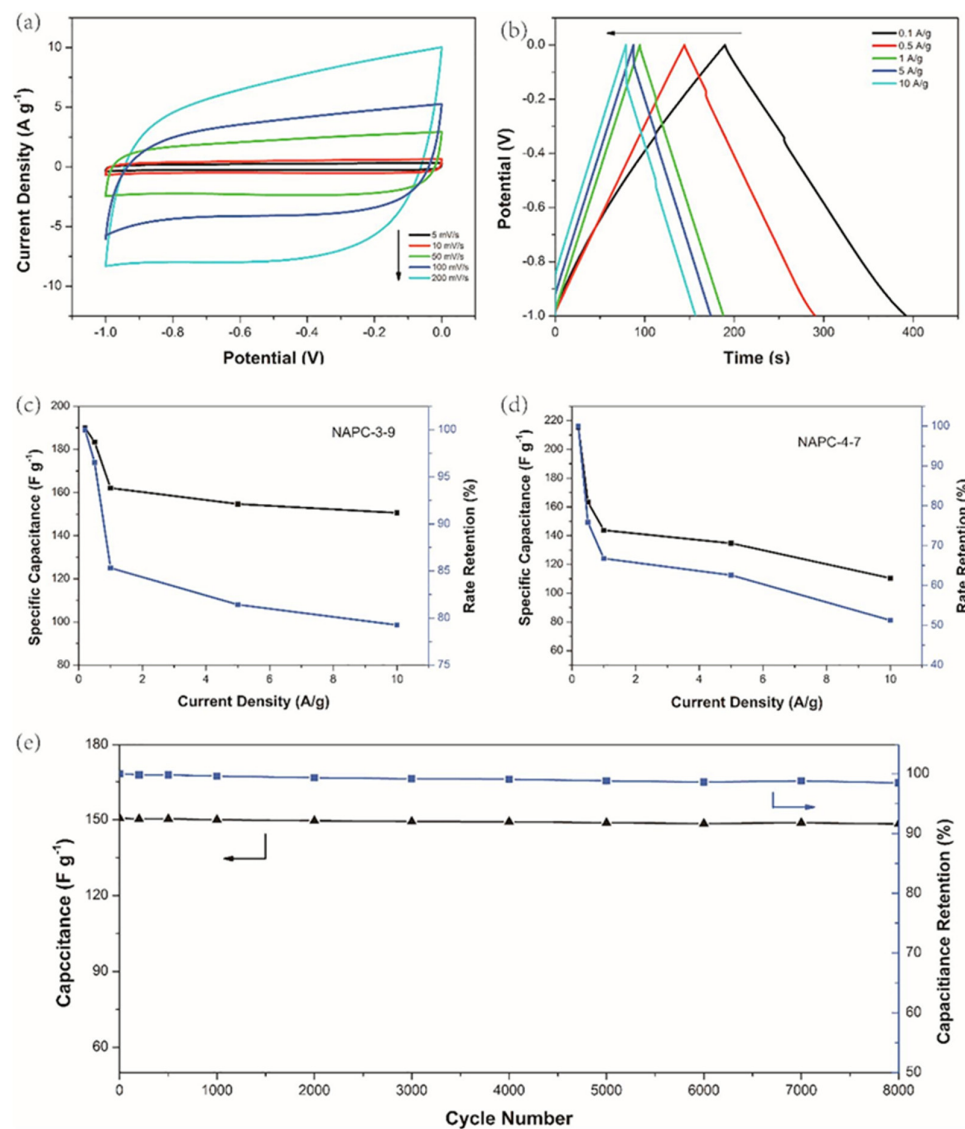


**Figure 21.** Electrochemical performance in symmetric supercapacitor system: (a,b) CV and charge–discharge curves for NAPC-3-9; specific capacitance determined from galvanostatic charge–discharge at different current densities and rate retention for (c) NAPC-3-9 and (d) NAPC-4-7; (e) cycling stability of NAPC-3-9 at  $10 \text{ A g}^{-1}$  [72].

#### 4.9. Electrochemical Aspects of Development of Aryl Ether-Free Cross-Linked Polymer Membranes for Supercapacitors

Murugan et al. (2024) [74] explore the development of novel polymer-based supercapacitor materials by synthesizing cross-linked Cu-MOF-bridged polybenzoxazine membranes (PABz-co-Cu MOFs) covalently grafted with poly(imidazole-co-diphenylamine) (PIDPA) (Figures 22 and 23). This innovative approach aims to enhance both proton conductivity and capacitive performance, making the material suitable for dual applications in high-temperature polymer electrolyte membrane fuel cells (HT-PEMFCs) and supercapacitors.

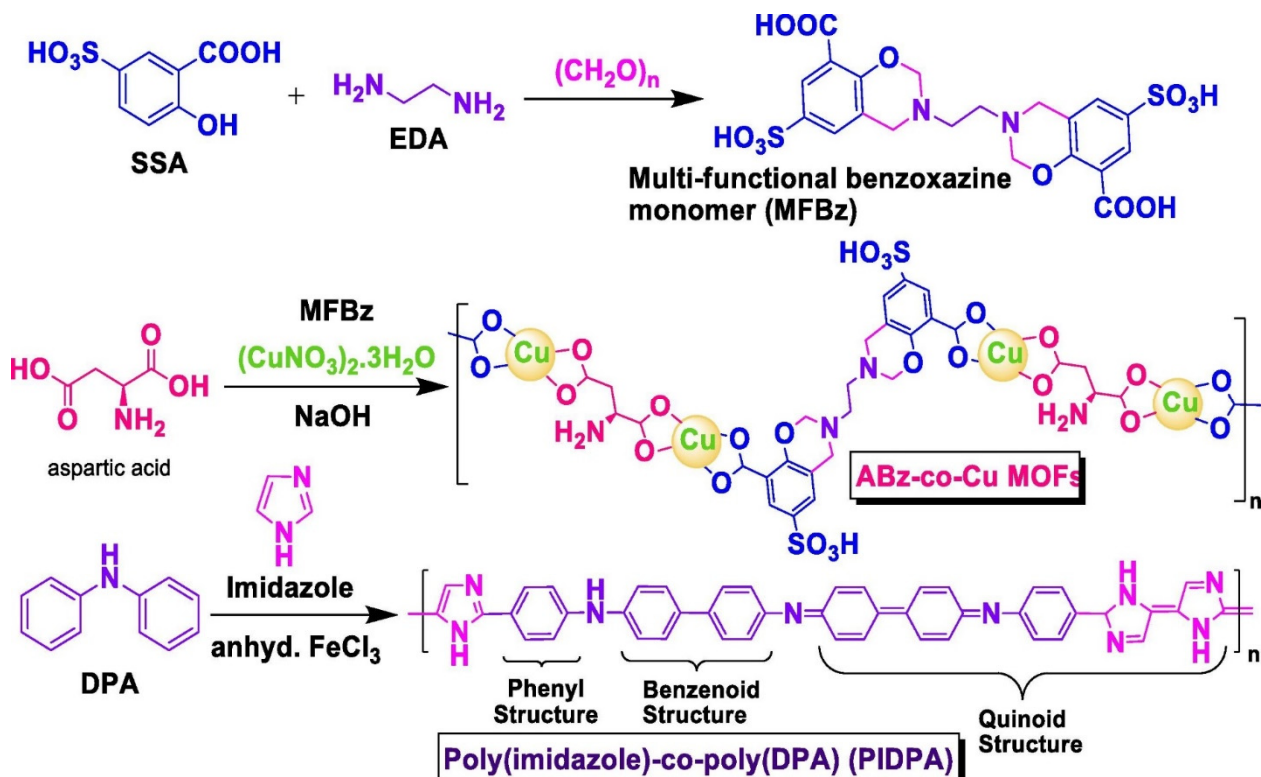


Figure 22. Diagram illustrating covalent cross-linking of PIDPA with PABz-co-Cu MOFs [74].

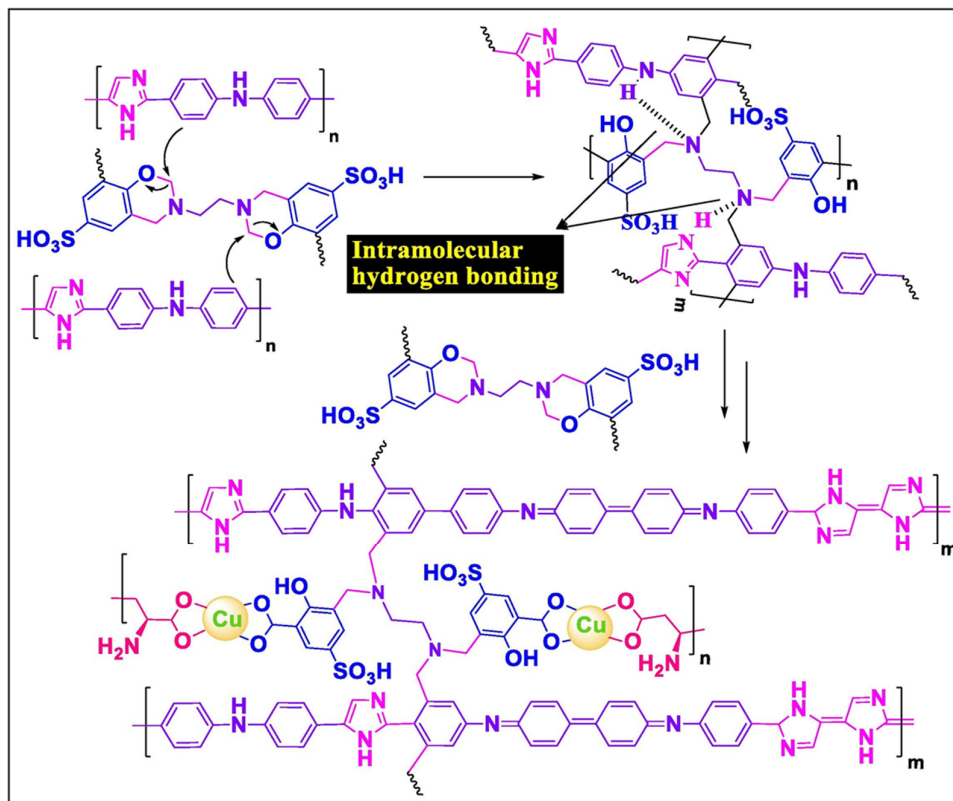
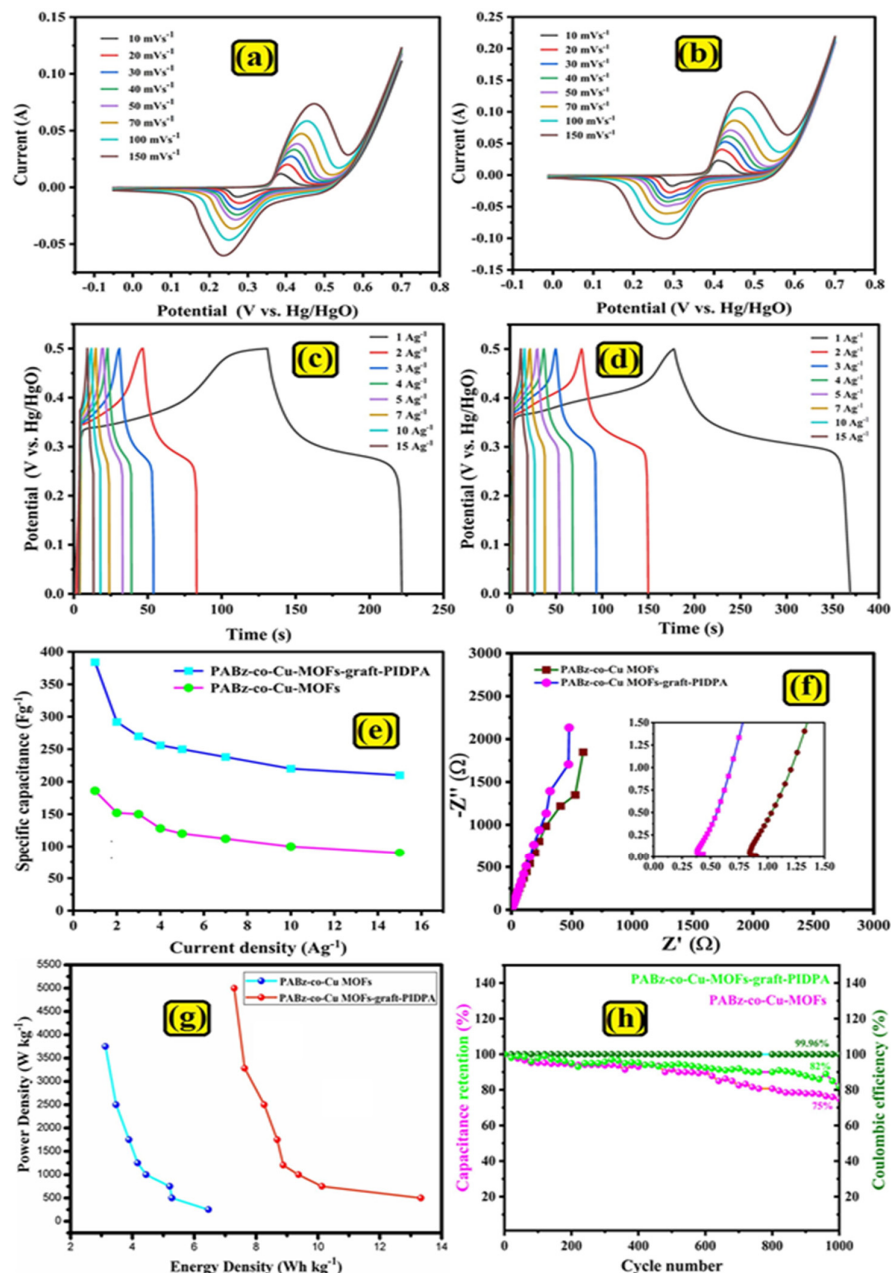


Figure 23. Scheme illustrating proposed reaction mechanism involving ABz-co-Cu MOFs and PIDPA, leading to formation of covalently cross-linked PABz-co-Cu MOFs-graft-PIDPA [74].

Cyclic voltammetry results indicate that the PA-doped PABz-co-Cu MOFs-graft-PIDPA membrane exhibits pronounced redox peaks, confirming its pseudocapacitive behavior.

(Figure 24a–h). The optimized 50/50 wt% composition achieves a remarkable specific capacitance of  $387 \text{ F g}^{-1}$  at  $1 \text{ A g}^{-1}$ , significantly outperforming the PABz-co-Cu MOFs alone, the specific capacitance of which only reaches  $187 \text{ F g}^{-1}$ . This enhancement is primarily attributed to the synergistic effects of metal–organic frameworks and conjugated polymer networks, which facilitate rapid charge transfer and increase the density of electrochemically active sites [74,75].



**Figure 24.** (a,b) CV, (c,d) GCD, (e) specific capacitance, (f) EIS curves (with zoomed-in high-frequency region inset), and (g) Ragone plots for PABz-co-Cu MOFs and 50/50% PABz-co-Cu MOFs-graft-PIDPA. (h) Specific capacitance retention of PABz-co-Cu MOFs and 50/50% cross-linked PABz-co-Cu MOFs-graft-PIDPA electrodes after 1000 cycles [74].

Galvanostatic charge–discharge measurements reveal a stable capacitance retention with minimal IR drop, indicative of high Coulombic efficiency. The polymer composite retains its electrochemical performance over prolonged cycling, underscoring its structural integrity and high reversibility. The combination of a metal–organic framework with

conductive polymer components enables a unique charge storage mechanism, leveraging both EDLC and pseudocapacitance contributions.

Electrochemical impedance spectroscopy analysis further validates the material's superior conductivity and low internal resistance. The incorporation of Cu-MOFs enhances electron mobility, while the nitrogen-rich polymer backbone improves ion transport. These attributes collectively contribute to a highly efficient charge storage system, making the PABz-co-Cu MOFs-graft-PIDPA membrane a promising candidate for next-generation energy storage applications. The study suggests further investigations into optimizing electrolyte compatibility and exploring hybrid configurations to push the performance boundaries of polymer-based supercapacitors [74,76].

#### 4.10. Electrochemical Aspects of Heteroatom-Enriched Carbon Particles for Supercapacitors

Tiwari et al. (2024) [77] focus on the development of heteroatom-enriched carbon particles derived from polybenzoxazine-based precursors for high-performance supercapacitor applications. This study highlights the significance of controlled molecular engineering to fabricate carbon structures with high nitrogen and oxygen doping, which enhances electrochemical properties crucial for supercapacitors. The work extensively examines the charge storage capabilities, stability, and capacitance retention of these materials, positioning them as strong contenders for next-generation energy storage solutions Figure 25.

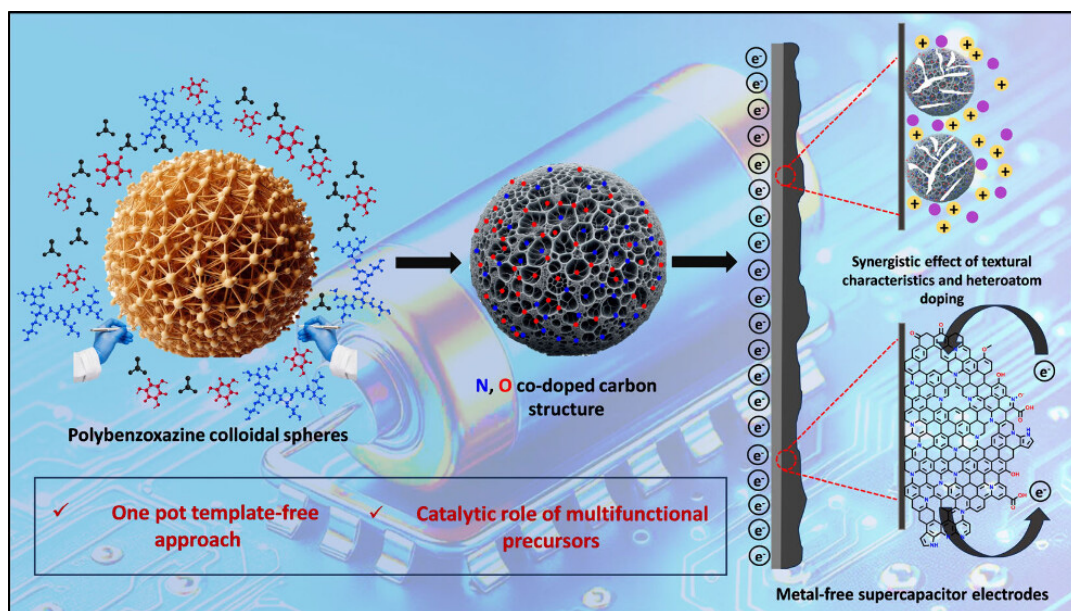


**Figure 25.** Diagram of heteroatom-doped carbon particles from multifunctional polybenzoxazine for enhanced supercapacitor performance [77].

The electrochemical performance of the synthesized heteroatom-doped carbon materials is investigated using CV, GCD, and impedance measurements (Figure 26A–H). The CV results demonstrate a quasi-rectangular shape, indicative of excellent capacitive behavior, with significant pseudocapacitive contributions from redox-active heteroatoms. The specific capacitance reaches an impressive 728 F/g at a current density of 10 A/g in 0.1 M H<sub>2</sub>SO<sub>4</sub> electrolyte, highlighting the material's high charge storage efficiency. Furthermore, GCD measurements confirm the material's rapid charge–discharge characteristics, displaying a high energy density of 56 Wh/kg and a power density of 14,246 W/kg [77,78]. EIS studies show low charge transfer resistance and improved ion diffusion, attributed to the hierarchical porous structure and the synergistic effects of nitrogen and oxygen doping. The electrode maintains 86% of its initial capacitance after 2500 cycles, demonstrating

excellent stability and reversibility. This remarkable performance positions heteroatom-enriched polybenzoxazine-derived carbons as promising electrode materials for advanced supercapacitor applications.

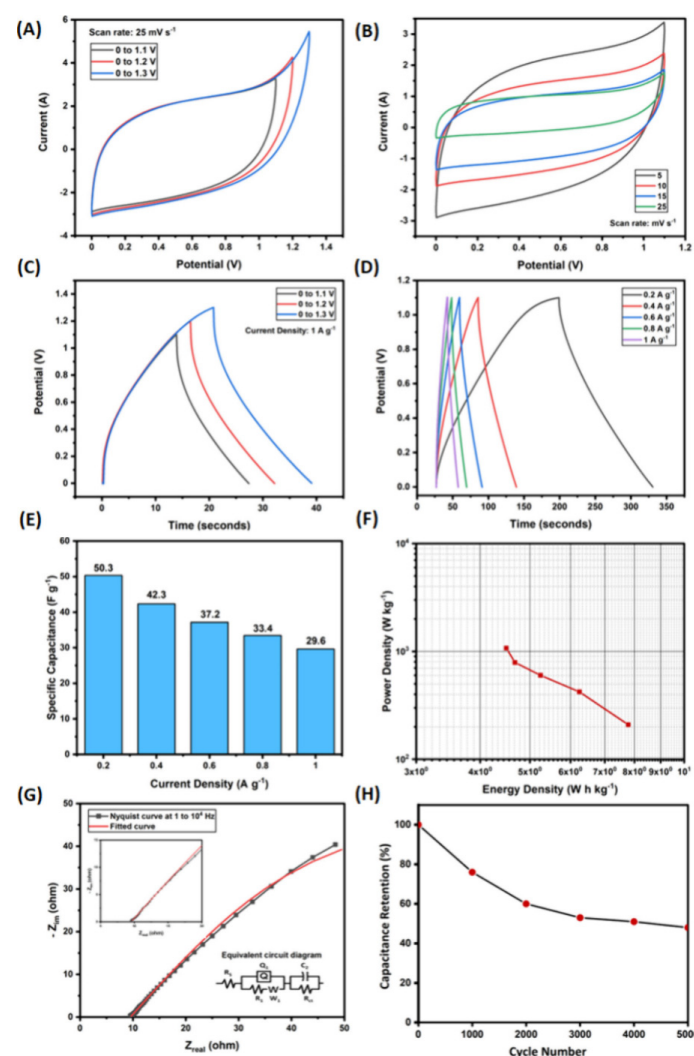


**Figure 26.** Electrochemical performance assessment of C–P–PEI in three-electrode system. **(A)** CV curves recorded at different potential windows with constant scan rate of 25 mV s<sup>-1</sup>. **(B)** CV curves measured at various scan rates within optimized potential window of −0.05 to 0.75 V. **(C)** GCD curves obtained at different current densities. **(D)** Specific capacitance (C<sub>sp</sub>) values calculated at 10 A g<sup>-1</sup> for varying current densities. **(E)** Breakdown of pseudocapacitance and EDLC contributions to total capacitance. **(F)** Ragone plot showing power density (P<sub>d</sub>) vs. energy density (E<sub>dsp</sub>). **(G)** Nyquist plot with inset highlighting midfrequency region. **(H)** Bode phase angle plot across frequency range of 1 to 10<sup>4</sup> Hz [77].

#### 4.11. Electrochemical Aspects of NRPC-Supported G-C<sub>3</sub>N<sub>4</sub>/Fe<sub>3</sub>O<sub>4</sub> for Supercapacitors

Selvaraj et al. (2024) [79] present a novel nitrogen-rich porous carbon (NRPC)-supported g-C<sub>3</sub>N<sub>4</sub>/Fe<sub>3</sub>O<sub>4</sub> nanocomposite for supercapacitor applications. The combination of NRPC with graphitic carbon nitride (g-C<sub>3</sub>N<sub>4</sub>) and magnetite (Fe<sub>3</sub>O<sub>4</sub>) aims to enhance conductivity, charge storage capacity, and cycling stability. The study systematically evaluates the electrochemical properties of the composite material and its potential for high-performance energy storage (Figure 27).

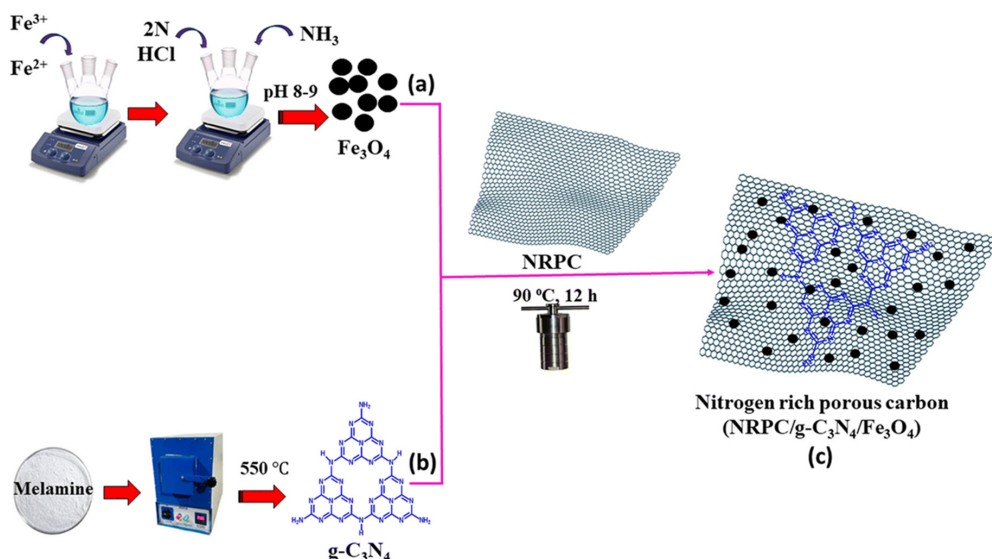


**Figure 27.** Diagram illustrating synthesis processes of (a)  $\text{Fe}_3\text{O}_4$  (magnetite), (b)  $\text{g-C}_3\text{N}_4$ , and (c) NRPC/g-C<sub>3</sub>N<sub>4</sub>/Fe<sub>3</sub>O<sub>4</sub> nanocomposites [79].

Cyclic voltammetry measurements (Figure 28) reveal significant redox activity, with the NRPC/g-C<sub>3</sub>N<sub>4</sub>/Fe<sub>3</sub>O<sub>4</sub> electrode exhibiting higher specific capacitance compared to pure  $\text{Fe}_3\text{O}_4$  and  $\text{g-C}_3\text{N}_4/\text{Fe}_3\text{O}_4$  electrodes. The material displays a combination of electric double-layer capacitance and pseudocapacitive behavior, contributing to its superior charge storage properties. The specific capacitance is determined to be 385 F/g at 1 A/g, outperforming  $\text{Fe}_3\text{O}_4$  (112 F/g) and  $\text{g-C}_3\text{N}_4/\text{Fe}_3\text{O}_4$  (150 F/g).

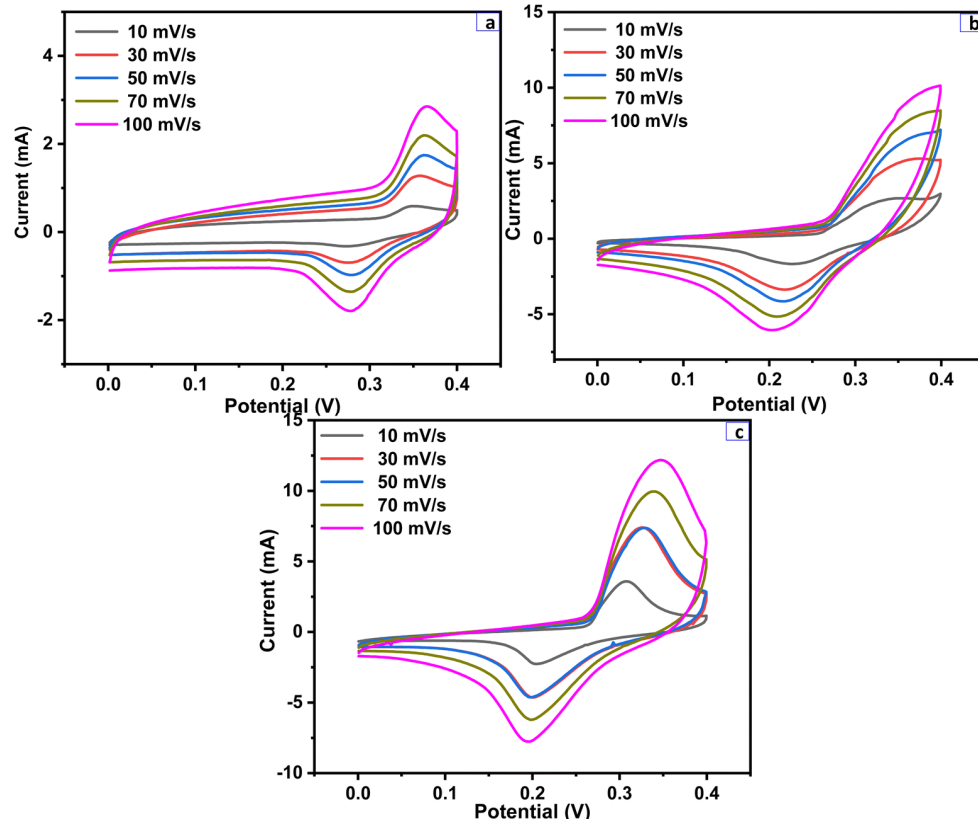


**Figure 28.** CV curves of (a)  $\text{Fe}_3\text{O}_4$ , (b)  $\text{g-C}_3\text{N}_4/\text{Fe}_3\text{O}_4$ , and (c) NRPC/g-C<sub>3</sub>N<sub>4</sub>/Fe<sub>3</sub>O<sub>4</sub> nanocomposites [79].

Galvanostatic charge–discharge studies (Figure 29) further validate the material’s efficiency, showing a retention of 94.3% capacitance after 2000 cycles at 5 A/g. The high cycling stability is attributed to the hierarchical porous architecture, which facilitates efficient electrolyte penetration and ion transport. Electrochemical impedance spectroscopy confirms lower charge transfer resistance, reinforcing the enhanced conductivity of the composite. The combination of NRPC with g-C<sub>3</sub>N<sub>4</sub> and Fe<sub>3</sub>O<sub>4</sub> significantly boosts electrochemical performance, making this material an excellent candidate for next-generation supercapacitor electrodes [79–82].

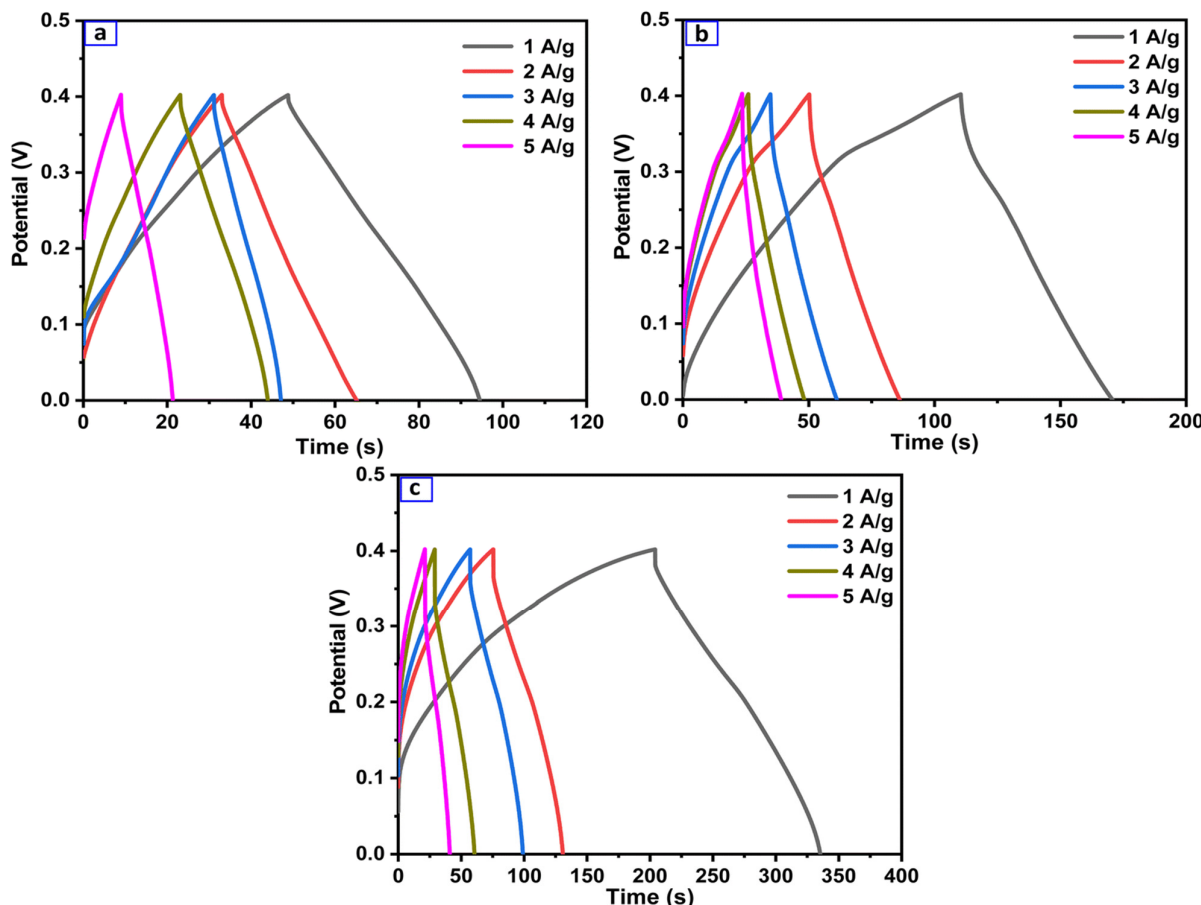


**Figure 29.** GCD curves for (a) Fe<sub>3</sub>O<sub>4</sub>, (b) g-C<sub>3</sub>N<sub>4</sub>/Fe<sub>3</sub>O<sub>4</sub>, and (c) NRPC/g-C<sub>3</sub>N<sub>4</sub>/Fe<sub>3</sub>O<sub>4</sub> nanocomposites [79].

#### 4.12. Electrochemical Aspects of LiFePO<sub>4</sub>@N-Doped Carbon for Lithium-Ion Batteries

Wang et al. (2016) [83] investigate the impact of nitrogen-doped carbon coatings derived from polybenzoxazine on the electrochemical performance of LiFePO<sub>4</sub> (LFP) cathodes for lithium-ion batteries (LIBs). The study aims to address the intrinsic limitations of LiFePO<sub>4</sub>, such as low electronic and ionic conductivity, by employing nitrogen-doped carbon to enhance charge transport and lithium-ion diffusion. The electrochemical performance of LiFePO<sub>4</sub>@N-doped carbon (LFP@NC) is characterized using cyclic voltammetry, galvanostatic charge–discharge, and electrochemical impedance spectroscopy (Figure 30a–d). CV studies demonstrate highly reversible redox peaks associated with the Fe<sup>2+</sup>/Fe<sup>3+</sup> redox couple, indicating enhanced electrochemical kinetics. The in situ nitrogen-doped carbon coating improves the conductivity of LiFePO<sub>4</sub>, leading to a significant reduction in charge transfer resistance.

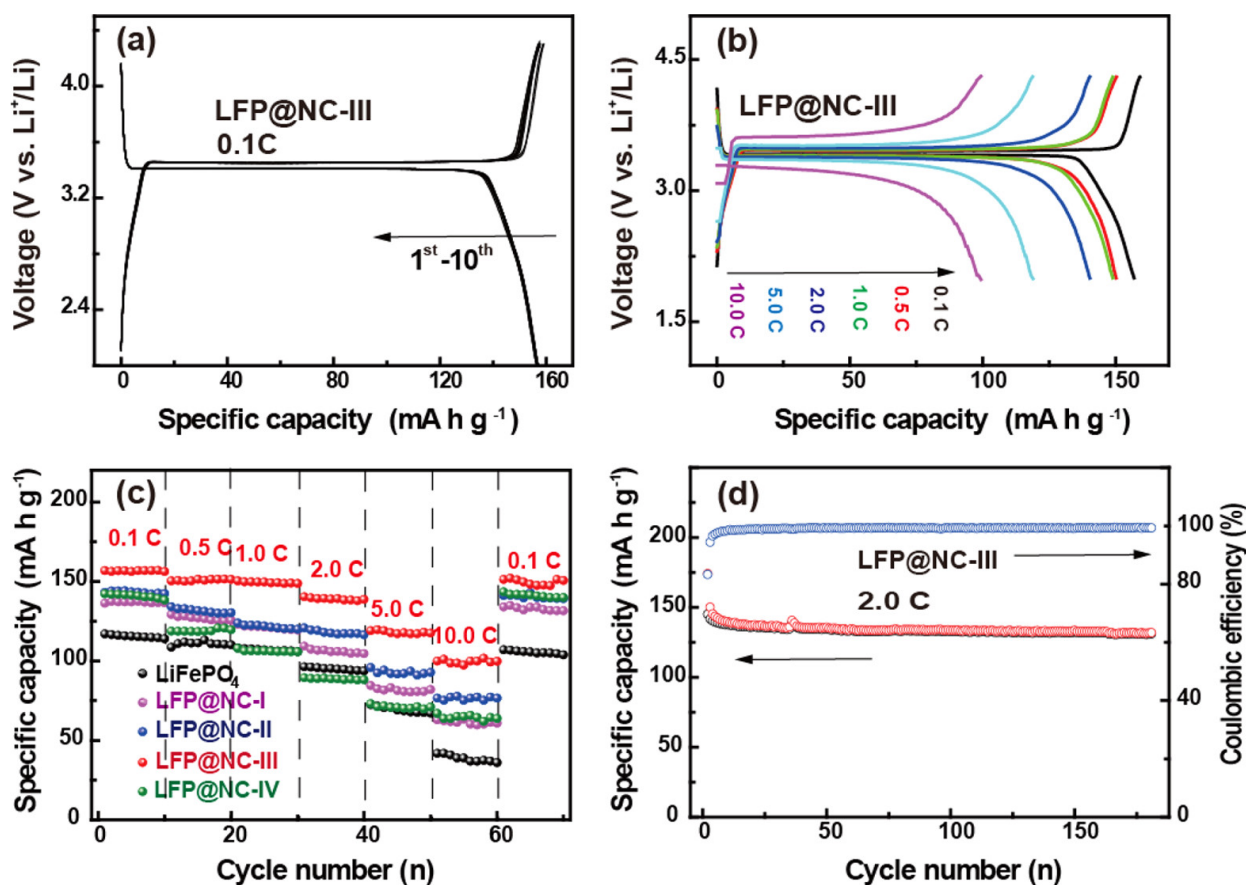


**Figure 30.** (a) Charge–discharge curves of LFP@NC-III nanocomposite electrode at 0.1 C for first 10 cycles. (b) Charge–discharge curves of LFP@NC-III electrode at various rates. (c) Comparison of rate performance between bare LiFePO<sub>4</sub> and LFP@NC at different rates. (d) Cycling performance and corresponding Coulombic efficiency of LFP@NC-III nanocomposite electrode at 2.0 C. All tests were conducted within voltage range of 2.0 to 4.3 V (vs. Li<sup>+</sup>/Li) [83].

Galvanostatic charge–discharge tests reveal that LFP@NC exhibits a specific capacitance of 156.9 mAh/g at 0.1 C, which is 1.34 times higher than that of bare LiFePO<sub>4</sub>. Even at high charge–discharge rates, the material maintains 63.7% of its initial capacity at 10 C, compared to only 34.7% for uncoated LiFePO<sub>4</sub>. This improvement is attributed to the nitrogen-doped carbon layer, which provides additional active sites for lithium-ion storage and facilitates rapid electron transport. Electrochemical impedance spectroscopy further confirms a substantial decrease in charge transfer resistance, demonstrating that the nitrogen-doped carbon coating effectively enhances the electrochemical kinetics of LiFePO<sub>4</sub>. The material retains 93.2% of its initial capacity after 180 cycles at 2 C, confirming its excellent long-term cycling stability. The integration of polybenzoxazine-derived nitrogen-doped carbon thus presents a viable strategy for improving lithium-ion battery performance [83,84].

#### 4.13. High-Ion-Conductivity Separator for Li-Ion Batteries Using Cross-Linked Polybenzoxazine

The study by Li et al. (2016) [85] highlights the potential of cross-linked polybenzoxazine electrospun fiber mats (CR-PBz-FbM) as high-performance separators for lithium-ion batteries, showcasing their superior ion conductivity, thermal stability, and electrolyte compatibility. The unique structure of CR-PBz-FbM, characterized by its highly porous morphology and strong molecular cross-linking, enables exceptional electrochemical performance, while ensuring dimensional integrity under extreme conditions (Figure 31). Given their ability to withstand high temperatures without degradation, PBz-derived materials

have garnered significant attention for use as precursors for porous carbon electrodes in supercapacitors, where thermal and electrochemical stability are critical for long-term operation.

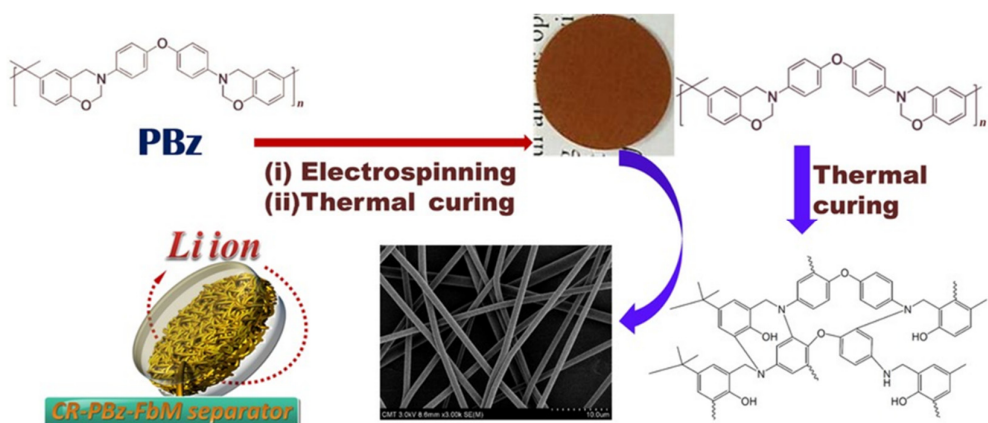


**Figure 31.** Chemical structure of PBz precursor and fabrication of CR-PBz-FbM electrospun fiber mat as separator for Li-ion batteries. SEM image illustrates fibers with diameter of 1.0 mm on sample following thermal-cross-linking process [85].

One of the defining features of PBz-derived materials is their high carbon yield upon pyrolysis, making them suitable for the fabrication of porous carbon electrodes with tunable microstructures. The CR-PBz-FbM separators developed by Li et al. exhibit an exceptionally high ion conductivity of  $2.92 \text{ mS cm}^{-1}$ , which is five times greater than conventional Celgard 2300 separators (Figure 32a–d). This enhanced performance is attributed to the material's high porosity (76%), which facilitates efficient ion transport, and its strong affinity for electrolytes, which improves wettability and charge transfer properties. Such features are particularly advantageous for supercapacitor applications, where the ability to maintain high charge–discharge efficiency and low internal resistance directly impacts energy storage capacity. Compared to other polymeric carbon precursors, such as polyacrylonitrile (PAN), phenolic resins, and cellulose-based materials, PBz offers a balanced combination of high-temperature stability, excellent electrochemical performance, and cost-effectiveness. The carbonization of PBz-based electrospun fiber mats results in highly interconnected porous networks that enhance ion diffusion and charge storage capabilities, making them a viable alternative for next-generation supercapacitor electrodes [86].

In addition to their remarkable electrochemical performance, PBz-derived carbon materials exhibit superior thermal stability compared to conventional polymer-based separators and electrodes. The study by Li et al. demonstrates that CR-PBz-FbM separators exhibit negligible shrinkage, even at  $150^\circ\text{C}$ , whereas commercial polyolefin-based separators undergo significant deformation at elevated temperatures. Furthermore, thermogravimetric analysis reveals that PBz-derived materials maintain structural integrity up to  $800^\circ\text{C}$  under nitrogen, with a residual carbon content exceeding 50%, indicating strong flame resistance and durability under harsh operating conditions. Such properties are critical for high-power supercapacitors, where stability at elevated temperatures and resistance to combustion are essential for ensuring safe and efficient energy storage. Moreover, the ability of PBz-derived carbon materials to be doped with heteroatoms such as nitrogen, oxygen, and phosphorus further enhances their electrochemical activity by introducing additional redox-active sites, thereby improving capacitance and charge–discharge cycling stability.

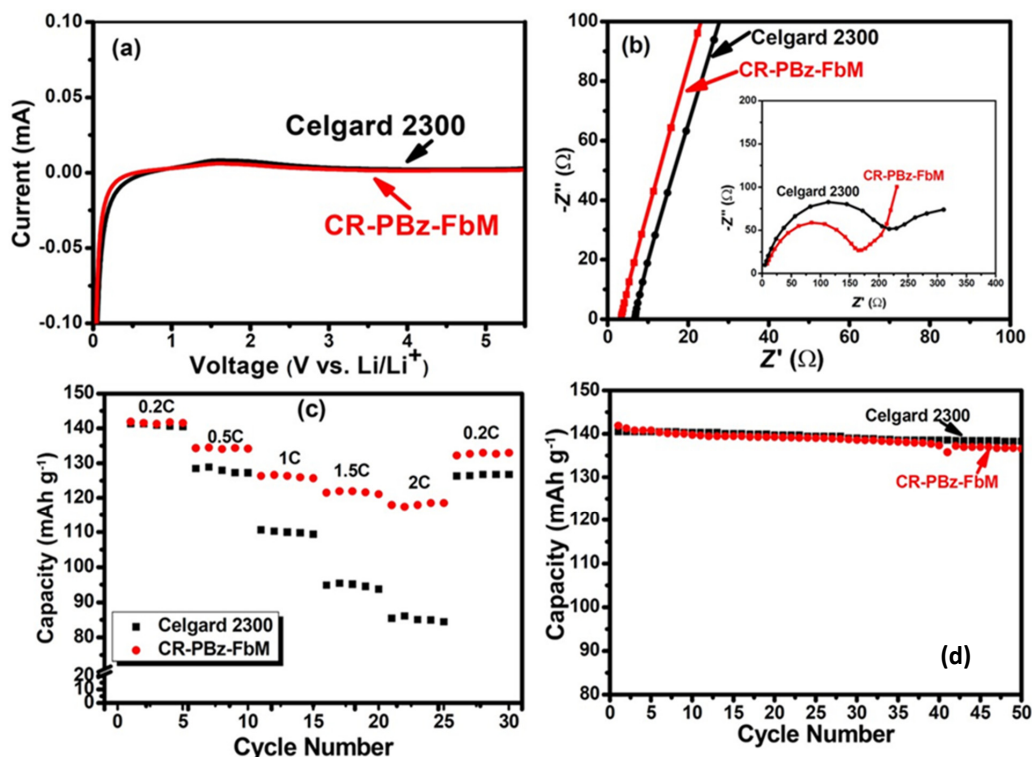


**Figure 32.** Electrochemical characterization and battery performance evaluation using  $\text{LiCoO}_2$ /separator/Li foil half-cells with CR-PBz-FbM separator. (a) Linear sweep voltammetry of CR-PBz-FbM and Celgard 2300 separators. (b) Nyquist plot representing AC impedance spectra of both separators. Inset: Nyquist plots for cells utilizing respective separators. (c) Rate capability tests for cells with different separators at various C-rates. (d) Cycling stability of cell using CR-PBz-FbM separator [85].

The versatility of polybenzoxazine-derived carbon materials extends beyond lithium-ion batteries and supercapacitors, with potential applications in fuel cells, electrocatalysis, and other advanced energy storage systems. Future research should focus on optimizing the carbonization process to tailor pore size distribution, surface area, and conductivity, as well as exploring hybrid materials that incorporate PBz-derived carbons with metal oxides or graphene to enhance charge storage capacity. Moreover, the development of scalable and cost-effective synthesis routes will be crucial in enabling the commercialization of PBz-based energy storage materials. The findings by Li et al. provide strong evidence that polybenzoxazine-derived materials hold immense promise as high-performance, thermally stable, and electrochemically efficient solutions for modern energy storage applications. As the demand for high-power, long-cycle-life, and environmentally sustainable supercapacitors continues to grow, the role of PBz-derived carbon materials in shaping the future of energy storage technologies cannot be overstated [87].

#### 4.14. Cross-Linked Polybenzoxazine Electrolytes for Enhanced Lithium Battery Cycling

A recent study by Wang et al. (2021) [88] explored cross-linked polybenzoxazine polymers incorporating poly(ethylene oxide) (PEO) segments, demonstrating their potential as solid polymer electrolytes for lithium-metal batteries. By enhancing ion transport, reducing crystallinity, and improving interfacial stability, these materials address some of the key limitations of conventional polymer electrolytes. This research provides a valuable foundation for understanding how PBz-derived carbon materials can be optimized for supercapacitor applications, particularly in enhancing electrochemical performance and stability under high-temperature conditions (Figure 33a–c).

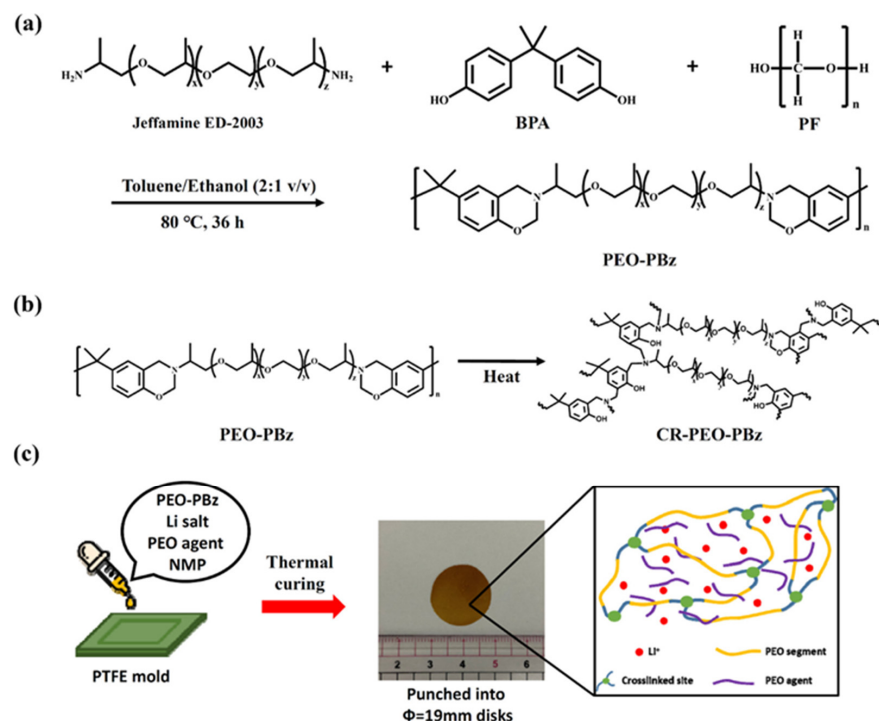


**Figure 33.** (a) Synthesis of PEO-PBz, (b) thermal cross-linking reaction of PEO-PBz to form CR-PEO-PBz, and (c) production of SPE using CR-PEO-PBz [88].

The thermal stability of polybenzoxazine-based materials is one of their most significant advantages. The study by Wang et al. demonstrated that cross-linked PEO-PBz (CR-PEO-PBz) structures suppress PEO crystallization, leading to an increased amorphous fraction that enhances lithium-ion transport. This effect is crucial not only for lithium-metal batteries, but also for supercapacitor electrodes, where ion diffusion and charge retention are key performance indicators. The CR-PEO-PBz materials in their study exhibited an ionic conductivity of  $5.32 \times 10^{-4} \text{ S cm}^{-1}$  at  $60^\circ\text{C}$ , a high electrochemical stability window exceeding 5.0 V, and the ability to suppress lithium dendrite formation over 700 h of cycling. These properties indicate that PBz-derived materials can serve as stable, high-performance carbon electrodes for supercapacitors by providing efficient charge transport channels and maintaining structural integrity under prolonged cycling (Figure 34a,b).

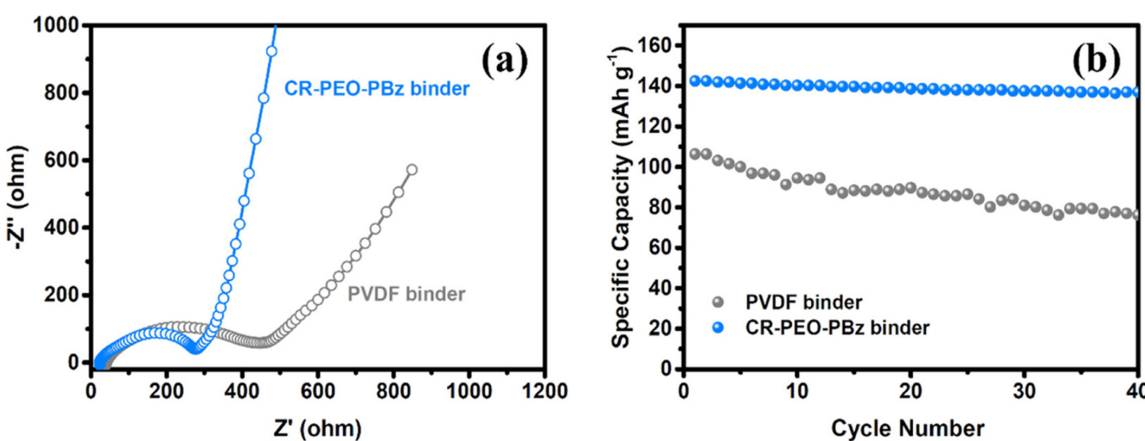


**Figure 34.** (a) Nyquist plots and (b) cycle tests performed on CR-PEO-PBz-based solid polymer electrolytes (containing 20 wt% PEO plasticizer and LiFSI salt) with varying binders (PVDF or CR-PEO-PBz) [88].

Another essential characteristic of PBz-derived carbon material is their high porosity and mechanical robustness, both of which are crucial for supercapacitor applications. The cross-linked PBz structure in Wang et al.'s study [88] demonstrated significant resistance to thermal decomposition up to 800 °C, ensuring a high residual char content and stability at elevated temperatures. In the context of supercapacitors, the porous nature of carbonized PBz materials enables a large electrolyte-accessible surface area, which is essential for achieving high specific capacitance. Additionally, the ability to functionalize PBz-based materials—such as by doping with nitrogen or oxygen—can further improve their pseudo-capacitive behavior, leading to enhanced charge storage capability. This aligns with recent advances in porous carbon electrodes, where materials with tailored pore architectures and heteroatom doping have demonstrated superior electrochemical performance [89].

Looking forward, the application of PBz-derived carbon materials in supercapacitors presents exciting possibilities for high-energy-density and thermally stable energy storage solutions. To optimize these materials for practical use, future research should focus on refining the carbonization process, improving electronic conductivity, and exploring composite architectures that combine PBz-based carbon with materials like graphene or transition metal oxides. Furthermore, strategies such as template-assisted synthesis or sol-gel processing could be employed to fine-tune the pore structure and surface chemistry of PBz-derived carbons. As demonstrated by Wang et al., PBz-based polymers offer a versatile platform for engineering high-performance, thermally stable materials, making them promising candidates for next-generation supercapacitors capable of operating under demanding conditions, while delivering exceptional charge storage efficiency [88–90]. Table 2 summarizes the electrochemical performance of various carbon-based materials, covering their capacitance, energy density, power density, and cycle stability.

**Table 2.** Electrochemical performance of various carbon-based materials, covering capacitance, energy density, power density, and cycle stability.

Material	Capacitance	Energy Density	Power Density	Cycle Stability
HC/NiCo@800 °C // HC [70]	232 F/g (using RbI electrolyte)	96.57 Wh/kg (using RbI electrolyte)	-	-
Porous carbon [72]	287.7 F/g (three-electrode), 190.0 F/g (two-electrode)	-	79.3% at 10 A/g	exceptional
PABz-co-Cu MOFs-graft-PIDPA [74]	387 F/g at 1 A/g	-	-	-
NP-rGO [59]	416 F/g	22.3 Wh/kg (at 500 W/kg)	-	94.63% capacitance maintained after 10,000 cycles
NRPC/g-C <sub>3</sub> N <sub>4</sub> /Fe <sub>3</sub> O <sub>4</sub> [79]	385 F/g at 1 A/g	-	-	94.3% after 2000 cycles
LFP@NC	-	-	favorable	stable
NRPC/NiMn [64]	1825 F/g	-	-	78% after 2500 cycles
Nitrogen-doped carbon [67]	700 F/g at 10 A/g	48 Wh/kg at 8400 W/kg	8400 W/kg	-
N, O-co-doped carbon [37]	728 F/g at 10 A/g	56 Wh/kg at 14,246 W/kg	14246 W/kg	86% capacitance retention after 2500 cycles
Porous carbon spheres [58]	344 F/g at 1 A/g	33.37 Wh/kg at 9000 W/kg	9000 W/kg	92% capacitance maintained after 5000 cycles

## 5. Conclusions and Perspective

Polybenzoxazine-derived carbon materials have emerged as promising candidates for advanced energy storage applications, due to their exceptional thermal stability, high carbon yield, tunable porosity, and superior electrochemical properties. This review has examined the structural evolution of these materials, their thermal degradation mechanisms,

and their performance in supercapacitor electrodes. Their diverse morphologies—ranging from aerogels to nanospheres—offer versatility in next-generation energy storage and multifunctional applications. The ability to maintain structural integrity under extreme thermal and electrochemical conditions further enhances their appeal for high-performance devices. Additionally, heteroatom doping with elements such as nitrogen, phosphorus, and sulfur has demonstrated significant improvements in charge storage capacity, ionic conductivity, and electrochemical stability, expanding their potential beyond conventional electric double-layer capacitors. Despite these advantages, several challenges remain in optimizing the synthesis, processing, and scalability of polybenzoxazine-derived carbon materials. One of the key limitations is the need for precise control over pore structure and surface chemistry to maximize electrochemical performance. Achieving an optimal balance between microporosity and mesoporosity is essential for improving ion accessibility and charge storage efficiency. Furthermore, the relatively high production cost of benzoxazine monomers and the complex polymerization process present barriers to large-scale commercialization. However, recent advances in cost-effective and sustainable synthesis approaches—such as biomass-derived benzoxazines, scalable template-assisted carbonization, and sol–gel processes—offer potential pathways to reduce costs and enhance material viability.

Scalability remains a crucial factor in the transition of polybenzoxazine-derived carbons from laboratory research to industrial applications. Traditional carbonization methods require high temperatures and controlled environments, increasing energy consumption and production costs. However, emerging techniques such as catalytic pyrolysis and solvent-free polymerization may lower energy requirements and improve yield efficiency. Preliminary cost analysis suggests that while benzoxazine monomers are more expensive than conventional carbon precursors, their high char yield and the possibility of tailored porosity at the nanoscale could offset costs by reducing material waste and enhancing performance efficiency. Additionally, integrating these materials into hybrid architectures—combining polybenzoxazine-based carbon with graphene, transition metal oxides, and metal–organic frameworks (MOFs)—could further enhance electrochemical performance, while improving cost-effectiveness. Beyond energy storage, polybenzoxazine-derived carbon materials hold great promise in gas adsorption, catalysis, electromagnetic shielding, and flame-retardant coatings. Their chemical resistance and high-temperature stability make them suitable for extreme environments, such as aerospace and defense applications. Furthermore, the development of flexible and lightweight polybenzoxazine-derived electrodes could revolutionize wearable electronics and portable power systems. In conclusion, polybenzoxazine-derived carbon materials offer a unique combination of thermal stability, tunable porosity, and excellent electrochemical performance, making them highly attractive for next-generation energy storage devices. Continued innovation in material design, synthesis strategies, and hybrid systems will be critical to overcoming current challenges and unlocking these materials' full potential in commercial and research applications. By leveraging advancements in nanotechnology, sustainable chemistry, and scalable manufacturing, these materials could play a transformative role in shaping the future of sustainable energy storage solutions.

**Author Contributions:** Conceptualization—T.P. and S.P.A.; methodology—T.P. and S.P.A.; validation—J.L.; formal analysis—T.P. and S.P.A.; investigation—J.L.; resources—J.L.; data curation—T.P. and S.P.A.; writing—original draft preparation—T.P. and S.P.A.; writing—review and editing—S.P.A., T.P. and J.L.; visualization—J.L.; supervision—J.L.; project administration—J.L.; funding acquisition—J.L. All authors have read and agreed to the published version of the manuscript.

**Funding:** This research received no external funding.

**Conflicts of Interest:** The authors declare no conflict of interest.

## References

1. Geim, A.K.; Novoselov, K. The rise of graphene. *Nat. Mater.* **2007**, *6*, 183–191. [[PubMed](#)]
2. Hummers, W.S., Jr.; Offeman, R.E. Preparation of Graphitic Oxide. *J. Am. Chem. Soc.* **1958**, *80*, 1339.
3. Iijima, S. Helical microtubules of graphitic carbon. *Nature* **1991**, *354*, 56–58.
4. Kroto, H.W.; Heath, J.R.; O'Brien, S.C.; Curl, R.F.; Smalley, R.E. C<sub>60</sub>: Buckminsterfullerene. *Nat. Cell Biol.* **1985**, *318*, 162–163.
5. Osawa, E.; Kroto, H.W.; Fowler, P.W.; Wasserman, E. The evolution of the football structure for the C<sub>60</sub> molecule: A retrospective. *Philos. Trans. R. Soc. London Ser. A Phys. Eng. Sci.* **1993**, *343*, 8.
6. Zhou, Y.; Chen, G.; Zhang, J. A review of advanced metal-free carbon catalysts for oxygen reduction reactions towards the selective generation of hydrogen peroxide. *J. Mater. Chem. A* **2020**, *8*, 20849–20869.
7. Tiwari, A. *Advanced Carbon Materials and Technology*; Wiley-Scrivener: Beverly, MA, USA, 2013.
8. Paul, R.; Dai, L. Interfacial aspects of carbon composites. *Compos. Interfaces* **2018**, *25*, 539–605.
9. McCreery, R.L. Advanced Carbon Electrode Materials for Molecular Electrochemistry. *Chem. Rev.* **2008**, *108*, 2646–2687.
10. Feng, L.; Zhang, W.X. The structure and magnetism of graphene. *AIP Adv.* **2012**, *2*, 042138.
11. Gaddam, R.R.; Kumar, N.A.; Narayan, R.; Raju, K.; Zhao, X. Advanced carbon materials for electrochemical energy storage. *Nanomater. Synth.* **2019**, *2019*, 385–418.
12. Ghosh, N.; Kiskan, B.; Yagci, Y. Polybenzoxazines—New high performance thermosetting resins: Synthesis and properties. *Prog. Polym. Sci.* **2007**, *32*, 1344–1391. [[CrossRef](#)]
13. Ishida, H. Overview and historical background of polybenzoxazine research. In *Handbook of Benzoxazine Resins*; Ishida, H., Agag, T., Eds.; Elsevier: Amsterdam, The Netherlands, 2011; pp. 3–81.
14. Ishida, H.; Froimowicz, P. (Eds.) *Advanced and Emerging Polybenzoxazine Science and Technology*; Elsevier: Amsterdam, The Netherlands, 2017.
15. Khan, J.; Momin, S.A.; Mariatti, M. A review on advanced carbon-based thermal interface materials for electronic devices. *Carbon* **2020**, *168*, 65–112.
16. Kiskan, B. Adapting benzoxazine chemistry for unconventional applications. *React. Funct. Polym.* **2018**, *129*, 76–88. [[CrossRef](#)]
17. Lyu, Y.; Ishida, H. Natural-sourced benzoxazine resins, homopolymers, blends and composites: A review of their synthesis, manufacturing and applications. *Prog. Polym. Sci.* **2019**, *99*, 101168.
18. Antil, B.; Elkasabi, Y.; Strahan, G.D.; Wal, R.L.V. Development of Graphitic and Non-Graphitic Carbons Using Different Grade Biopitch Sources. *Carbon* **2025**, *232*, 119770. [[CrossRef](#)]
19. Asrafali, S.P.; Periyasamy, T.; Lee, J. High-Performance Supercapacitors Using Compact Carbon Hydrogels Derived from Polybenzoxazine. *Gels* **2024**, *10*, 509. [[CrossRef](#)]
20. Shah, S.S.; Aziz, M.A.; Marzooqi, M.A.; Khan, A.Z.; Yamani, Z.H. Enhanced Light-Responsive Supercapacitor Utilizing BiVO<sub>4</sub> and Date Leaves-Derived Carbon: A Leap towards Sustainable Energy Harvesting and Storage. *J. Power Sources* **2024**, *602*, 234334. [[CrossRef](#)]
21. Zhen, H.; Yang, H.; Wang, M.; Lu, G.; Liu, Y.; Run, M. Cyclo-oligomerization of hydroxyl-containing mono-functional benzoxazines: A mechanism for oligomer formation. *Polym. Chem.* **2020**, *11*, 2325–2331. [[CrossRef](#)]
22. Zhang, K.; Liu, Y.; Ishida, H. Polymerization of an AB-type benzoxazine monomer toward different polybenzoxazine networks: When diels–alder reaction meets benzoxazine chemistry in a single-component resin. *Macromolecules* **2019**, *52*, 7386–7395. [[CrossRef](#)]
23. Wang, Y.; Gawryla, M.D.; Schiraldi, D.A. Effects of freezing conditions on the morphology and mechanical properties of clay and polymer/clay aerogels. *J. Appl. Polym. Sci.* **2013**, *129*, 1637–1641. [[CrossRef](#)]
24. Trybuła, D.; Marszałek-Harych, A.; Gazińska, M.; Berski, S.; Jedrzkiewicz, D.; Ejfler, J. N-Activated 1,3-Benzoxazine Monomer as a Key Agent in Polybenzoxazine Synthesis. *Macromolecules* **2020**, *53*, 8202–8215. [[CrossRef](#)] [[PubMed](#)]
25. Sini, N.K.; Endo, T. Toward Elucidating the Role of Number of Oxazine Rings and Intermediates in the Benzoxazine Backbone on Their Thermal Characteristics. *Macromolecules* **2016**, *49*, 8466–8478.
26. Ohashi, S.; Ishida, H. Various synthetic methods of benzoxazine monomers. In *Advanced and Emerging Polybenzoxazine Science and Technology*; Ishida, H., Froimowicz, P., Eds.; Elsevier: Amsterdam, The Netherlands, 2017; pp. 3–8.
27. Kistler, S.S. Coherent Expanded Aerogels and Jellies. *Nat. Cell Biol.* **1931**, *127*, 741.
28. Han, L.; Salum, M.L.; Zhang, K.; Froimowicz, P.; Ishida, H. Intrinsic self-initiating thermal ring-opening polymerization of 1,3-benzoxazines without the influence of impurities using very high purity crystals. *J. Polym. Sci. Part A Polym. Chem.* **2017**, *55*, 3434–3445.
29. Fung, A.; Wang, Z.; Lu, K.; Dresselhaus, M.; Pekala, R. Characterization of carbon aerogels by transport measurements. *J. Mater. Res.* **1993**, *8*, 1875–1885.

30. Cui, S.; Arza, C.R.; Froimowicz, P.; Ishida, H. Developing further versatility in benzoxazine synthesis via hydrolytic ring-opening. *Polymers* **2020**, *12*, 694. [[CrossRef](#)]
31. Cheng, Z.; DeGracia, K.; Schiraldi, D.A. Sustainable, low flammability, mechanically-strong poly(vinyl alcohol) aerogels. *Polymers* **2018**, *10*, 1102. [[CrossRef](#)]
32. Lorjai, P.; Chaisuwan, T.; Wongkasemjit, S. Porous structure of polybenzoxazine-based organic aerogel prepared by sol–gel process and their carbon aerogels. *J. Sol-Gel Sci. Technol.* **2009**, *52*, 56–64.
33. Mahadik-Khanolkar, S.; Donthula, S.; Sotiriou-Leventis, C.; Leventis, N. Polybenzoxazine aerogels. 1. High-yield room temperature acid-catalyzed synthesis of robust monoliths, oxidative aromatization, and conversion to microporous carbons. *Chem. Mater.* **2014**, *26*, 1303–1317.
34. Sun, M.; Sun, H.; Wang, Y.; Sanchez-Soto, M.; Schiraldi, D.A. The relation between the rheological properties of gels and the mechanical properties of their corresponding aerogels. *Gels* **2018**, *4*, 33. [[CrossRef](#)]
35. Thubsuang, U.; Ishida, H.; Wongkasemjit, S.; Chaisuwan, T. Self-formation of 3D interconnected macroporous carbon xerogels derived from polybenzoxazine by selective solvent during the sol–gel process. *J. Mater. Sci.* **2014**, *49*, 4946–4961. [[CrossRef](#)]
36. Haozhe, X.; Haibo, F.; Ya, L. Preparation and Characterization of Carbon Aerogel Based on MainChain Benzoxazine. *ACS Appl. Eng. Mater.* **2024**, *2*, 116–125.
37. Tiwari, I.; Tanwar, V.; Ingole, P.P.; Nebhani, L. Heteroatom-Enriched Carbon Particles Derived from Multifunctional Polybenzoxazine Particles for High-Performance Supercapacitors. *ACS Appl. Energy Mater.* **2024**, *7*, 7185–7204. [[CrossRef](#)]
38. Ma, Q.; Wang, H.; Zhan, G.; Liu, X.; Yang, Y.; Zhuang, Q.; Qian, J. Preparing Multifunctional High-Performance Cross-Linked Polybenzoxazole Aerogels from Polybenzoxazine. *ACS Appl. Polym. Mater.* **2021**, *3*, 2352–2362. [[CrossRef](#)]
39. Si, Y.; Ren, T.; Li, Y.; Ding, B.; Yu, J. Fabrication of magnetic polybenzoxazine-based carbon nanofibers with  $\text{Fe}_3\text{O}_4$  inclusions with a hierarchical porous structure for water treatment. *Carbon* **2012**, *50*, 5176–5185. [[CrossRef](#)]
40. Thubsuang, U.; Ishida, H.; Wongkasemjit, S.; Chaisuwan, T. Advanced and economical ambient drying method for controlled mesopore polybenzoxazine-based carbon xerogels: Effects of non-ionic and cationic surfactant on porous structure. *J. Colloid Interface Sci.* **2015**, *459*, 241–249. [[CrossRef](#)]
41. Zhu, Y.; Jiang, Y.; Lin, R.; Yu, S. Research on thermal degradation process of p-nitrophenol-based polybenzoxazine. *Polym. Degrad. Stab.* **2017**, *141*, 1–10. [[CrossRef](#)]
42. Zhu, Y.; Gu, Y. Effect of interaction between transition metal oxides and nitrogen atoms on thermal stability of polybenzoxazine. *J. Macromol. Sci. Part B* **2011**, *50*, 1130–1143.
43. Speight, J.G. Industrial Organic Chemistry. In *Environmental Organic Chemistry for Engineers*; Elsevier: Amsterdam, The Netherlands, 2017; pp. 87–151.
44. Low, H.Y.; Ishida, H. Structural effects of phenols on the thermal and thermo-oxidative degradation of polybenzoxazines. *Polymer* **1999**, *40*, 4365–4376.
45. Low, H.Y.; Ishida, H. Improved thermal stability of polybenzoxazines by transition metals. *Polym. Degrad. Stab.* **2006**, *91*, 805–815.
46. Low, H.Y.; Ishida, H. An investigation of the thermal and thermo-oxidative degradation of polybenzoxazines with a reactive functional group. *J. Polym. Sci. Part B Polym. Phys.* **1999**, *37*, 647–659.
47. Liu, Y.; Zhang, H.; Wang, M.; Liao, C.; Zhang, J. Thermal degradation behavior and mechanism of polybenzoxazine based on bisphenol-S and methylamine. *J. Therm. Anal. Calorim.* **2013**, *112*, 1213–1219.
48. Liu, Y.; Yue, Z.; Li, Z.; Liu, Z. Thermal degradation behavior and kinetics of polybenzoxazine based on bisphenol-S and aniline. *Thermochim. Acta* **2011**, *523*, 170–175.
49. Huang, S.; Gu, J.; Ye, J.; Fang, B.; Wan, S.; Wang, C.; Ashraf, U.; Li, Q.; Wang, X.; Shao, L.; et al. Benzoxazine monomer derived carbon dots as a broad-spectrum agent to block viral infectivity. *J. Colloid Interface Sci.* **2019**, *542*, 198–206.
50. Hemvichian, K.; Laobuthee, A.; Chirachanchai, S.; Ishida, H. Thermal decomposition processes in polybenzoxazine model dimers investigated by TGA–FTIR and GC–MS. *Polym. Degrad. Stab.* **2002**, *76*, 1–15.
51. Hemvichian, K.; Ishida, H. Thermal decomposition processes in aromatic amine-based polybenzoxazines investigated by TGA and GC–MS. *Polymer* **2002**, *43*, 4391–4402.
52. Hamerton, I.; Thompson, S.; Howlin, B.J.; Stone, C.A. New method to predict the thermal degradation behavior of polybenzoxazines from empirical data using structure property relationships. *Macromolecules* **2013**, *46*, 7605–7615.
53. Fang, B.; Lu, X.; Hu, J.; Zhang, G.; Zheng, X.; He, L.; Cao, J.; Gu, J.; Cao, F. pH controlled green luminescent carbon dots derived from benzoxazine monomers for the fluorescence turn-on and turn-off detection. *J. Colloid Interface Sci.* **2019**, *536*, 516–525.
54. Bagherifam, S.; Uyar, T.; Ishida, H.; Hacaloglu, J. The use of pyrolysis mass spectrometry to investigate polymerization and degradation processes of methyl amine-based benzoxazine. *Polym. Test.* **2010**, *29*, 520–526.
55. Zhao, J.; Gilani, M.R.H.S.; Lai, J.; Nsabimana, A.; Liu, Z.; Luque, R.; Xu, G. Autocatalysis Synthesis of Poly(Benzoxazine-Co-Resol)-Based Polymer and Carbon Spheres. *Macromolecules* **2018**, *51*, 5494–5500.
56. Zhang, R.; Wang, L.; Zhao, J.; Guo, S. Effects of Sodium Alginate on the Composition, Morphology, and Electrochemical Properties of Electrospun Carbon Nanofibers as Electrodes for Supercapacitors. *ACS Sustain. Chem. Eng.* **2019**, *7*, 632–640.

57. Zhao, J.; Niu, W.; Zhang, L.; Cai, H.; Han, M.; Yuan, Y.; Majeed, S.; Anjum, S.; Xu, G. A Template-Free and Surfactant-Free Method for High-Yield Synthesis of Highly Monodisperse 3- Aminophenol-Formaldehyde Resin and Carbon Nano/Microspheres. *Macromolecules* **2013**, *46*, 140–145.
58. Xue, D.; Zhu, D.; Xiong, W.; Cao, T.; Wang, Z.; Lv, Y.; Li, L.; Liu, M.; Gan, L. Template-Free, Self-Doped Approach to Porous Carbon Spheres with High N/O Contents for High-Performance Supercapacitors. *ACS Sustain. Chem. Eng.* **2019**, *7*, 7024–7034.
59. Cheng, H.; Yi, F.; Gao, A.; Liang, H.; Shu, D.; Zhou, X.; He, C.; Zhu, Z. Supermolecule Self-Assembly Promoted Porous N, P Co-Doped Reduced Graphene Oxide for High Energy Density Supercapacitors. *ACS Appl. Energy Mater.* **2019**, *2*, 4084–4091.
60. Chen, Z.; Chen, Y.; Wang, Q.; Yang, T.; Luo, Q.; Gu, K.; Yang, W. Molecularly-Regulating Oxygen-Containing Functional Groups of Ramie Activated Carbon for High-Performance Supercapacitors. *J. Colloid Interface Sci.* **2024**, *665*, 772–779.
61. Si, Y.; Ren, T.; Ding, B.; Yu, J.; Sun, G. Synthesis of mesoporous magnetic Fe<sub>3</sub>O<sub>4</sub>@carbon nanofibers utilizing in situ polymerized polybenzoxazine for water purification. *J. Mater. Chem.* **2012**, *22*, 4619–4622.
62. Huang, Z.; Pan, Q.; Smith, D.M.; Li, C.Y. Plasticized Hybrid Network Solid Polymer Electrolytes for Lithium-Metal Batteries. *Adv. Mater. Interfaces* **2019**, *6*, 1801445.
63. Zhang, J.; Li, J.-Y.; Wang, W.-P.; Zhang, X.-H.; Tan, X.-H.; Chu, W.-G.; Guo, Y.-G. Microemulsion Assisted Assembly of 3D Porous S Graphene G-C3N4 Hybrid Sponge as. *Adv. Energy Mater.* **2018**, *8*, 1702839.
64. Periyasamy, T.; Asrafali, S.P.; Kim, S.C. Nitrogen-Rich Porous Carbon/NiMn Hybrids as Electrode Materials for High-Performance Supercapacitors. *ACS Appl. Energy Mater.* **2022**, *5*, 15605–15614.
65. Shaer, C.; Oppenheimer, L.; Lin, A.; Ishida, H. Advanced Carbon Materials Derived from Polybenzoxazines: A Review. *Polymers* **2021**, *13*, 3775. [CrossRef]
66. Ma, X.; Ning, G.; Qi, C.; Xu, C.; Gao, J. Phosphorus and Nitrogen Dual-Doped Few-Layered Porous Graphene: A High-Performance Anode Material for Lithium-Ion. *Batteries* **2014**, *6*, 14415–14422. [CrossRef] [PubMed]
67. Sharma, P.; Tanwar, V.; Tiwari, I.; Ingole, P.P.; Nebhani, L. Sustainable Upcycling of Nitrogen-Enriched Polybenzoxazine Thermosets into Nitrogen-Doped Carbon Materials for Contriving High-Performance Supercapacitors. *Energy Fuels* **2023**, *37*, 7445–7467. [CrossRef]
68. Liu, J.; Ishida, H. Anomalous Isomeric Effect on the Properties of Bisphenol F-Based Benzoxazines: Toward the Molecular Design for Higher Performance. *Macromolecules* **2014**, *47*, 5682–5690. [CrossRef]
69. Yu, Z.; Yu, W.; Jiang, Y.; Wang, Z.; Zhao, W.; Liu, X. Upcycling of Polybenzoxazine to Magnetic Metal Nanoparticle-Doped Laser-Induced Graphene for Electromagnetic Interference Shielding. *ACS Appl. Nano Mater.* **2022**, *5*, 13158–13170. [CrossRef]
70. Asrafali, S.P.; Periyasamy, T.; Kim, S.C. Enhanced Electrochemical Performance of HC/NiCo@ 800 C //HC Using Redox-Active Electrolytes Showing Increased Energy Density. *J. Alloys Compd.* **2024**, *972*, 172753. [CrossRef]
71. Zhuang, X.; Zhang, F.; Wu, D.; Zhuang, X.F. Graphene Coupled Schiff-base Porous Polymers Towards Nitrogen-enriched Porous Carbon. *Adv. Mater.* **2014**, *26*, 3081–3086. [CrossRef]
72. Wang, J.; Zhang, P.; Liu, L.; Zhang, Y.; Yang, J.; Zeng, Z.; Deng, S. Controllable Synthesis of Bifunctional Porous Carbon for Efficient Gas-Mixture Separation and High-Performance Supercapacitor. *Chem. Eng. J.* **2018**, *348*, 57–66.
73. Cao, J.; Han, Y.; Zheng, X.; Wang, Q. Preparation and Electrochemical Performance of Modified Ti<sub>3</sub>C<sub>2</sub>T<sub>x</sub>/Polypyrrole Composites. *J. Appl. Polym. Sci.* **2019**, *136*, 47003. [CrossRef]
74. Murugan, E.; Munusamy, K.; Vallipparambil Babu, A. Development of Aryl Ether-Free Cross-Linked Polymer Membranes for Sustainable Electrochemical Energy Conversion and Storage Applications. *Chem. Eng. J.* **2024**, *501*, 157473.
75. Devadas, B.; Imae, T. Effect of Carbon Dots on Conducting Polymers for Energy Storage Applications. *ACS Sustain. Chem. Eng.* **2018**, *6*, 127–134.
76. Yao, Z.; Erhong, S.; Wei, C.; Carlo, U.S.; Zhou, J.; Yung-Chang, L.; Zhu, C.; Ma, R.; Liu, P.; Chu, S.; et al. Dual-Metal Interbonding as the Chemical Facilitator for Single-Atom Dispersions. *Adv. Mater.* **2020**, *32*, 2003484.
77. Ertas, Y.; Uyar, T. Main-chain polybenzoxazine nanofibers via electrospinning. *Polymer* **2014**, *55*, 556–564.
78. Ting, F.Y.; Lingna, S.X.H.; Fanfan, W.Y.Z.; Ying, X. Approaching High-Performance Lithium Storage Materials by Constructing. *Energy Environ. Mater.* **2021**, *4*, 586–595.
79. Selvaraj, K.; Yu, B.; Spontón, M.E.; Kumar, P.; Veerasamy, U.S.; Arulraj, A.; Mangalaraja, R.V.; Almarhoon, Z.M.; Sayed, S.R.M.; Kannaiyan, D. Nonylphenol Polybenzoxazines-Derived Nitrogen-Rich Porous Carbon (NRPC)-Supported g-C<sub>3</sub>N<sub>4</sub>/Fe<sub>3</sub>O<sub>4</sub> Nanocomposite for Efficient High-Performance Supercapacitor Application. *Soft Matter* **2024**, *20*, 7957–7969.
80. Bheema, R.K.; Verma, A.; Bhaskaran, K.; Etika, K.C. A Review on Recent Progress in Polymer Composites for Effective Electromagnetic Interference Shielding Properties- Structures, Process, Sustainability Approaches. *Nanoscale Adv.* **2024**, *6*, 5773–5802.
81. Zu, G.; Wang, X.; Kanamori, K.; Nakanishi, K. Superhydrophobic Highly Flexible Doubly Cross-Linked Aerogel/Carbon Nanotube Composites as Strain/Pressure Sensors. *J. Mater. Chem. B* **2020**, *8*, 4883–4889.

82. Ananthanarayanan, A.; Wang, Y.; Routh, P.; Sk, M.A.; Than, A.; Lin, M.; Zhang, J.; Chen, J.; Sun, H.; Chen, P. Nitrogen and Phosphorus Co-Doped Graphene Quantum Dots: Synthesis from Adenosine Triphosphate, Optical Properties, and Cellular Imaging. *Nanoscale* **2015**, *7*, 8159–8165.
83. Wang, P.; Zhang, G.; Li, Z.; Sheng, W.; Zhang, Y.; Gu, J.; Zheng, X.; Cao, F. Improved Electrochemical Performance of LiFePO<sub>4</sub>@N-Doped Carbon Nanocomposites Using Polybenzoxazine as Nitrogen and Carbon Sources. *ACS Appl. Mater. Interfaces* **2016**, *8*, 26908–26915.
84. El-Shinawi, H.; Cussen, E.J.; Corr, S.A. Morphology-Directed Synthesis of LiFePO<sub>4</sub> and LiCoPO<sub>4</sub> from Nanostructured Li<sub>1+2X</sub>PO<sub>3-X</sub>. *Inorg. Chem.* **2019**, *58*, 6946–6949.
85. Li, H.-Y.; LI, G.-A.; Lee, Y.-Y.; Tuan, H.-Y.; Liu, Y.-L. A Thermally Stable Combustion-Resistant and Highly Ion-Conductive Separator for Lithium-Ion. *Energy Technol.* **2016**, *4*, 551–557.
86. Wu, Z.-S.; Winter, A.; Chen, L.; Sun, Y.; Turchanin, A.; Feng, X.; Müllen, K. Three-Dimensional Nitrogen and Boron Co-doped Graphene for High-Performance. *Adv. Mater.* **2012**, *24*, 5130–5135. [PubMed]
87. Raul, D.; Shchadenko, R.S.; Murastov, G.; Lipovka, A.; Fatkullin, M.; Petrov, I.; Tran, T.-H.; Khalelov, A.; Saqib, M.; Villa, N.E.; et al. Ultra-Robust Flexible Electronics by Laser-Driven Polymer-Nanomaterials. *Adv. Funct. Mater.* **2021**, *31*, 2008818.
88. Wang, T.C.; Tsai, C.Y.; Liu, Y.L. Solid Polymer Electrolytes Based on Cross-Linked Polybenzoxazine Possessing Poly(Ethylene Oxide) Segments Enhancing Cycling Performance of Lithium Metal Batteries. *ACS Sustain. Chem. Eng.* **2021**, *9*, 6274–6283.
89. Krüner, B.; Schreiber, A.; Tolosa, A.; Quade, A.; Badaczewski, F.; Pfaff, T.; Smarsly, B.M.; Presser, V. Nitrogen-Containing Novolac-Derived Carbon Beads as Electrode Material for Supercapacitors. *Carbon* **2018**, *132*, 220–231.
90. Zhao, N.; Wu, S.; He, C.; Shi, C.; Liu, E.; Du, X.; Li, J. Hierarchical Porous Carbon with Graphitic Structure Synthesized by a Water Soluble Template Method. *Mater. Lett.* **2012**, *87*, 77–79.

**Disclaimer/Publisher's Note:** The statements, opinions and data contained in all publications are solely those of the individual author(s) and contributor(s) and not of MDPI and/or the editor(s). MDPI and/or the editor(s) disclaim responsibility for any injury to people or property resulting from any ideas, methods, instructions or products referred to in the content.